CHALMERS

High gain waveguide slot array antenna for 60 GHz point-to-point communication

Thesis for the degree of Master of Science in Wireless, Photonics and Space Engineering

FARID HADAVY

Department of Signals and Systems
CHALMERS UNIVERSITY OF TECHNOLOGY
Gothenburg, Sweden, 2014

Thesis for the degree of Master of Science in Wireless, Photonics and Space Engineering

High gain waveguide slot array antenna for 60GHz point-to-point communication

FARID HADAVY

Department of Signals and Systems
CHALMERS UNIVERSITY OF TECHNOLOGY
Gothenburg, Sweden, 2014

High gain waveguide slot array antenna for 60 GHz point-to-point communication

FARID HADAVY

Chalmers university of technology
Department of Signals and Systems
SE-412 96 Göteborg
Sweden
Telephone + 46(0) 31-772 1000

Printed by Chalmers Reportservice
Göteborg, Sweden, 2014

High gain waveguide slot array antenna for 60 GHz point-to-point communication

FARID HADAVY
Department of Signals and Systems
CHALMERS UNIVERSITY OF TECHNOLOGY

Abstract

The 7GHz license free allocated frequency band around 60GHz is very attractive for both indoors and outdoors communication such as 4G/LTE backhaul, wireless Gigabit Ethernet bridges, next generation Gigabit Wi-Fi and HD transmitter etc. Due to the high path loss at this frequency band, for outdoor point-to-point links, high gain antennas are essential to compensate for the losses. In this thesis the planar waveguide slot arrays has been investigated and a high gain double layer array has been designed and simulated. As part of the work, in order to enhance the bandwidth, different slot and waveguide shapes such as trapezoid and half-ridge slots have been simulated. But wide rectangular slots combined with short subarrays showed best result and were therefore used in the design of the final double layer antenna. The designed antenna is a 128×128 array with H-plane T-junction power divider network in the bottom layer. The antenna showed a gain o 45.5dBi over the entire band of interest, namely from 57-64GHz and had an overall efficiency of 63%.The cross-polarization discrimination is -43dB.

Keywords: planar slot array, 60 GHz point-to point link, high gain antenna

Acknowledgment

I would like to sincerely thank my supervisor and examiner Jian Yang (Associate Professor) for his guidance, invaluable discussions and suggestions and most of all for giving me the opportunity to do my thesis in the department of signals and systems and working on the subject that interested me the most.

I would thank my fiancé, Fereshte for her unstoppable support during my education. She believed in me and gave me the energy and self-confidence that helped me all the way. Words are short to express my gratitude towards her.

Contents

Chapter 1

Introduction

Point-to-point communication links operating at 60GHz, mostly used for Gigabit Ethernet bridges in local area networks (LAN), has gained popularity for the last decade due to the large allocated license free frequency band around 60GHz. Due to the high path loss of electromagnetic waves at 60GHz, utilizing high gain antennas are necessary for the system to function [1]. Reflector antennas are commonly employed for this kind of systems but this type of antennas are heavy and bulky. Another drawback for reflector antennas at high frequencies is the requirement on the surface roughness which complicates the manufacturing. Flat, light and highly efficient array antennas that have potential for cost effective mass production are very attractive at millimeter wave frequencies[1].

1.1 Purpose

The purpose of this work is to investigate the performance of waveguide slot array antenna and design a high gain antenna for 60GHz point-to-point communication links to meet specification.

1.2 Thesis outline

In chapter 2 the basic theories and technology backgrounds are presented and the relevant equations are given and briefly discussed. The design of the antenna is carried out by first investigating the performance of a simple slot array and learning the limit on the array length. Then a simple single layer slot array antenna with integrated H-plane power divider was investigated theoretically to see if a partially traveling and partially standing wave solution can fulfill the requirements. Finally a double layer antenna was designed; simulation and dissuasion about all the antenna components can be found in chapter 3. In chapter 3 some other slot and waveguide shapes that presumed to enhance the bandwidth have also been investigated and discussed. In chapter 4 the fabrication of the antenna and the possibility of integrating a diplexer are discussed. In addition the

gain enhancement through enlargement of the antenna size is briefly discussed in this chapter. Final conclusions are summarized in chapter 5.

Chapter 2

Basic theory and technology background

In this chapter the relevant theories of the antenna and its components are presented and important equations are listed.

2.1 Antenna characterization

2.1.1 Directivity

The directivity of an antenna is defined as "the ratio of the radiation intensity in a given direction from the antenna to the radiation intensity averaged over all directions"[2] and is given by the equation 2.1.1.

$$D = \frac{U}{U_0} = \frac{4\pi U}{P_{rad}} \quad (2.1.1)$$

where U is radiation intensity, U_0 is the radiation intensity of an isotropic source and P_{rad} is the total radiated power and is given by equation 2.1.2.

$$P_{rad} = \frac{1}{2}\oiint U\, d\Omega = \int_0^{2\pi}\int_0^{\pi} U sin\theta d\theta d\varphi \quad (2.1.2)$$

The radiation intensity U is a function of the far-zone electric field according to equation 2.1.3[2].

$$U(\theta,\varphi) \cong \frac{1}{2\eta}\left[\left|E_\theta{}^{r=0}(\theta,\varphi)\right|^2 + \left|E_\varphi{}^{r=0}(\theta,\varphi)\right|^2\right] \quad (2.1.3)$$

2.1.2 Bandwidth

Antenna characteristics such as directivity, polarization, input impedance, sidelobe level etc. usually vary with frequency. The frequency band within which these characteristics have acceptable values compared to those at the center

frequency, defines the bandwidth of the antenna. The characterization of the antenna bandwidth however is not unique because the antenna characteristics do not vary in the same fashion. Two bandwidth definitions are used in order to organize the characteristics better, the impedance bandwidth which is related to input impedance and radiation efficiency, and the pattern bandwidth which includes polarization, beamwidth, gain and sidelobe level[3].

2.2 Planar broadside array antenna of equally spaced elements

Planar array can provide high directivity and compact size at the same time and are attractive in many applications. The normalized array factor of a planar array with M and N elements along the x-axis and y-axis respectively, and with uniform amplitude excitation, is given by equation 2.2.1.

$$AF_n(\theta,\varphi) = \left\{\frac{\sin\left(\frac{M\psi_x}{2}\right)}{\mathrm{M}\sin\left(\frac{\psi_x}{2}\right)}\right\}\left\{\frac{\sin\left(\frac{N\psi_y}{2}\right)}{\mathrm{N}\sin\left(\frac{\psi_y}{2}\right)}\right\} \quad (2.2.1)$$

where

$$\psi_x = kd_x sin\theta cos\varphi + \beta_x$$

$$\psi_y = kd_y sin\theta sin\varphi + \beta_y$$

In the equation 2.2.1, d_x and d_y are the element spacing and β_x and β_y are the progressive phase shifts between the elements along x and y-axis respectively.
For uniform array with the elements spacing d_x and d_y less than λ the grating lobs in both x-z and y-z planes are avoided [4]. In order to have broadside (normal to the plane of antenna elements) radiation, the progressive phase shifts should be zero.

2.2.1 Directivity of the planar array

The directivity of a planar array is given by the equation 2.2.2

$$D = e_{grating} e_{pol} e_{ill} \cos\theta_0 \, D_{max} \quad (2.2.2)$$

Where the first three terms are grating lobe, polarization and illumination efficiencies respectively and θ_0 is the steered angle from broadside. D_{max} is maximum available directivity of the aperture of the array and is given by equation 2.2.3.

$$D_{max} = \frac{4\pi A}{\lambda^2} \quad (2.2.3)$$

Where A is the aperture area [5].

For a planar array which has its main beam along broadside direction and no grating lobes, the equation 2.2 can be reduced to equation 2.2.4.

$$D = e_{pol}\, D_{max} \quad (2.2.4)$$

Another useful measure of the antenna performance is the antenna gain which takes into account the directional capabilities as well as the efficiency. The antenna gain is closely related to the directivity according to equation 2.2.5[5].

$$G(\theta, \varphi) = e_{conduction} e_{dielectric} D(\theta, \varphi) \quad (2.2.5)$$

2.3 Rectangular waveguide

A rectangular waveguide is a type of transmission line that supports TE and TM waves and is used in many applications including millimeter wave and high power systems. The dominant mode is TE_{10} and it is often desired that only this mode propagates in the waveguide. The cutoff frequency of the TE_{10} is given by equation 2.3.1[4].

$$f_{c10} = \frac{1}{2a\sqrt{\mu\epsilon}} \quad (2.3.1)$$

Where a is the large dimension of the waveguide and μ and ϵ are the permeability and permittivity of the material filling the waveguide.

The transverse field components of the TE_{10} are given by equation 2.3.2-4.

$$H_y = E_x = 0 \quad (2.3.2)$$

$$E_y = \frac{-j\omega\mu a}{\pi} A_{10} sin\frac{\pi x}{a} e^{-j\beta_{10} z} \quad (2.3.3)$$

$$H_x = \frac{-j\beta_{10} a}{\pi} A_{10} sin\frac{\pi x}{a} e^{-j\beta_{10} z} \quad (2.3.4)$$

where β_{10} is the propagation constant of the TE_{10} mode and is given by 2.3.5.

$$\beta_{10} = \sqrt{\omega^2\epsilon\mu - (\frac{\pi}{a})^2} \quad (2.3.5)$$

The guided wavelength differs from free space wavelength and is given by 2.3.6.

$$\lambda_{g10} = \frac{2\pi}{\beta_{10}} = \frac{2\pi}{\sqrt{\omega^2\epsilon\mu - (\frac{\pi}{a})^2}} = \frac{\lambda}{\sqrt{1 - (\frac{\lambda}{2a})^2}} > \lambda \quad (2.3.6)$$

The attenuation for TE_{10} due to the conductor loss is treated by perturbation method and is given by equation 2.3.7.

$$\alpha_c = \frac{R_s}{a^3 b \beta_{10} k \eta}(2b\pi^2 + a^3 k^2) \quad (2.3.7)$$

where R_s is the wall surface resistance and $\eta = \sqrt{\frac{\mu}{\epsilon}}$ is the wave impedance of the dielectric material filling the waveguide which is η =377 Ohm for the air filled waveguide[4].

The surface current of density for all modes can be found from the magnetic field intensity H on the wall according to equation 2.3.8.

$$J = a_n \times H \quad (2.3.8)$$

where thea_n is the unit vector normal to the wall. For TE_{10} mode and at the center of the broad wall the two components of the surface current are given by 2.3.9-10[6].

$$J_x = H_z = -jsin\frac{\pi x}{a}e^{-j\beta_{10}z} \quad (2.3.9)$$

$$J_z = H_x \quad (2.3.10)$$

2.4 Ridge rectangular waveguide

Ridge waveguide is commonly used in broadband microwave equipments. Ridge waveguides have higher operation bandwidth compared to conventional rectangular waveguides due to larger separation between the dominant mode and first order modes. The impedance of the ridge waveguide is lower than the rectangular waveguide, which is desirable in many applications for better matching. The ridge rectangular waveguide consists of a rectangular waveguide with one or more ridge inserted. Figure 2.1 illustrates single and double ridge waveguide geometries [7].

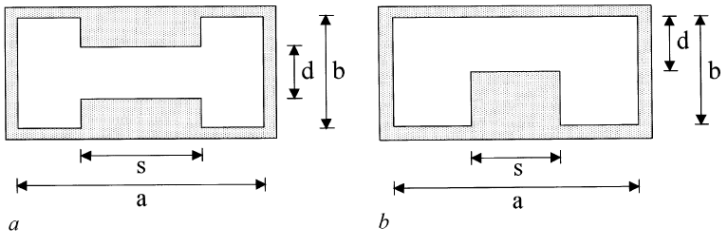

Figure 2.1 Single (b) and double (a) rectangular ridge waveguide geometries [8]

Another interesting property of ridge waveguide is that the cut-off wavelength can be changed by adjusting details of the ridge.

The cut-off space of single and double ridge waveguides have been analyzed by different method such as *finite element method* (FEM) and *mode matching method* (MMM). In the figure 2.2 and 2.3 the cut-off space of single and double rectangular ridge waveguide are shown respectively [8].

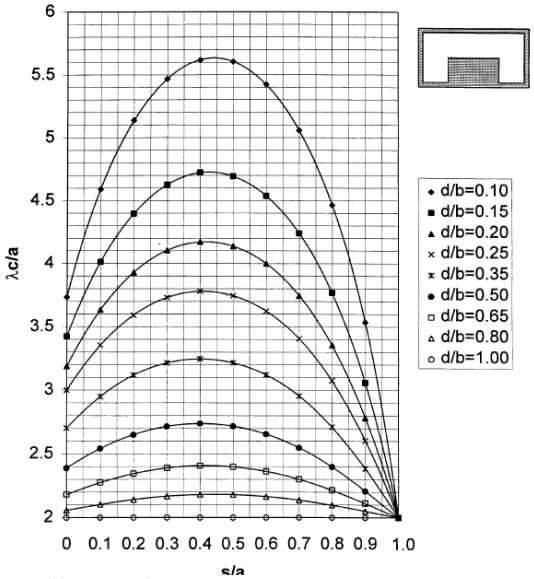

Figure2.2 Cut-off space of the single ridge waveguide (*b/a =0.45*) [8]

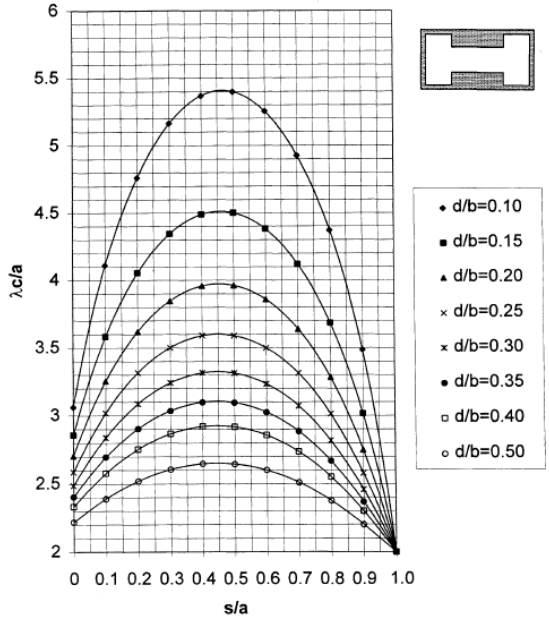

Figure 2.3 Cut-off space of double ridge waveguide (*b/a =0.45*) [8]

2.5 Slot antenna

Slots in a metallic ground plane are used commonly as radiators due to their low cost and accuracy in manufacturing. Arrays of longitudinal rectangular slots in waveguide walls are very common and are employed in many different areas. The theories and expression presented here is mainly for this type of slot.

2.5.1 Field distribution and radiation pattern

A rectangular slot in an infinite PEC (perfect electric conductor) ground plane is actually a small rectangular waveguide and therefore the fields inside the slot are the same as a rectangular waveguide with the same dimensions. For a slot with a narrow profile and a length about half a wavelength, the TE_{10} mode dominates and equations 2.3.2-4 can be used to find the fields components [9].

The radiation pattern from a slot with arbitrary shape is similar to a dipole antenna with the same shape and dimension but with the E-and H-plane interchanged according to Babinet's principle [10]. The ground plane in the slot antennas makes the field behind $\theta = \frac{\pi}{2}$ zero and therefore the directivity of a half wave slot is 5.17dBi which is twice of that of the half wave dipole in free space [9].

2.5.2 Slot in a waveguide wall

A longitudinal rectangular slot usually is modeled by a shunt admittance, the normalized admittance is evaluated from the calculated or measured reflection coefficient Γ according to equation 2.4.1 [11].

$$\frac{Y}{Y_0} = \frac{-2\,\Gamma}{1+\,\Gamma} \qquad (2.4.1)$$

The shunt admittance model is a simple model with good accuracy only at the resonance frequency of the slot; a more accurate model however is presented by an equivalent T-network as shown in the figure 2.4.1.

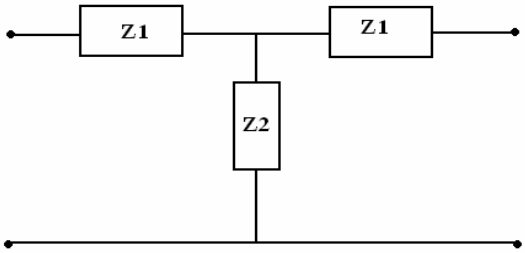

Figure 2.4.1 Equivalent T-network of a longitudinal slot [11]

The impedances Z_1 and Z_2 can be calculated from the reflection and transmission coefficients and are given by equations 2.4.2-3 [11].

$$Z_1 = \frac{1 + \Gamma - T}{1 - \Gamma + T} \quad (2.4.2)$$

$$Z_2 = \frac{2T}{(1 - \Gamma + T)(1 + \Gamma - T)} \quad (2.4.3)$$

The normalized radiation conductance for a single slot in broad wall of a rectangular waveguide, as can be seen in the approximated equation 2.4.4 [10], is a function of the slot displacement from the centerline of the wall d. Therefore by choosing appropriate slot displacement the array input impedance can be matched to the impedance of the transmission line and keep the input reflection low.

$$G_{rad} = \frac{2.1\, a\lambda_g}{b\lambda} cos^2\left(\frac{\pi\lambda}{2\lambda_g}\right) sin^2\left(\frac{\pi d}{a}\right) \quad (2.4.4)$$

For an array of slots, the radiation conductance of the slots are in parallel and thus adds up. Hence for a long array with lots of slots the radiation conductance of each slot should be small which simply means that the displacement from the center line should be small.

2.5.3 Array of slots in a waveguide wall (slotted waveguide array)

There are different configurations of slotted waveguide arrays but the common arrays are designed as resonance or traveling wave arrays. The resonant array utilizes a short-circuited end waveguide to produce the standing waves within the waveguide which feeds the slots uniformly with the same amplitude and phase (zero phase shifts between the array elements). The traveling wave arrays uses a matched load at the end of the waveguide to avoid the standing waves, in this configurations the slots displacements from the centerline must be optimized to feed the slots with uniform amplitude. In addition a linearly progressive phase shift appears between the slots which is desired/undesired depending on the specific application[9][10].

The resonant type usually has narrower bandwidth compared to the traveling wave type due to its dependence on the standing wave wavelength λ_g[9]. The bandwidth of the resonance array and methods for improvement, are discussed in the next subsection.

When designing array antennas it is important to have a good understanding of the mutual coupling between the elements. For a set of *N* elements array in a common ground plane an N-port linear system can be set up as in equation 2.4.5.

$$I_m = \sum_{n=1}^{N} V_n Y_{mn} \qquad (2.4.5)$$

Where I_m is the input current and Y_{mm} is the self-admittance at the *m*th slot, V_n is the applied voltage at the *n*th slot and Y_{mn} is the mutual impedance between the *m*th and *n*th slots. The relation between the admittance matrix of the slot array $[Y^s]$ and its impedance matrix of the complementary dipole array $[Z^d]$ is derived from Booker's relation and is given by equation 2.4.6.

$$[Y^s] = \frac{4}{\eta^2}[Z^d] \qquad (2.4.6)$$

Where η is the intrinsic impedance of the material in which the structure is immersed [12].

2.5.4 Bandwidth of slotted waveguide array

As mentioned earlier the resonant waveguide slot array is band limited and the usable bandwidth is only a few percent. This limitation is due to the frequency dependence of the slots and also the moving of the standing wave peaks from the slots locations by frequency [9][13].

One way to improve the bandwidth is to use slots with geometries that can provide larger bandwidth such as wide rectangular slots or so-called dumbbell slots. Using these geometries however makes a tradeoff between bandwidth improvement and cross-polar radiation degradation. Another way to enhance the bandwidth is to reduce the number of the slots per waveguide and use subarray instead. This is a possible solution because the problem with the phase variation caused by standing-wave movements gets worse with increasing the number of the slots (phase error grows with propagation length). The study of these two methods in [14] shows that the latter method is the most effective way to enhance the bandwidth of the slot array antenna. This method however requires an extra waveguide layer (for planar array) and thus increase the overall cost. The pattern performance (radiation pattern, gain etc.) was also compared in [14] for the case of longitudinal slots, wideband slots and subarray; the results shows that the pattern performance is not significantly affected when wideband solutions are used.

Chapter 3

Antenna design

The design of the antenna was carried out by first surveying some planar antennas for millimeter frequencies (>30GHz), especially, waveguide slot array antennas. After that the array dimensions were calculated. A short 4-slot array was designed and simulated to examine its performance and limitations. The shape of both the slots and waveguides were also discussed and new slot shapes that presumed to enhance the bandwidth were investigated briefly. In section 3.7 a high gain single layer waveguide slot array antenna was investigated, but the requirements could not be fulfilled by this antenna and therefore a double layer slot array antenna was finally designed. In section 3.8 each component of the double layer antenna was designed, simulated and discussed separately. Due to the complexity and large size of the final antenna, it was not possible to simulate the antenna in actual size. Instead an approximate approach, infinite array simulation, was employed to estimate the radiation characteristic and account for mutual coupling between elements; the losses for the antenna was analytically estimated.

3.1 Antenna specifications

The regulations and spectrum allocation for 60GHz band differs from country to country. An antenna bandwidth of 9GHz centered on 61.5GHz would however cover the entire band in any country (countries that allows unlicensed 60GHz communication). FCC (Federal communication commission) has recently updated the rules and now allows maximum ERIP of 85dBm (82dBm average ERIP) and a maximum RF power of 27dBm. FCC has however related the maximum allowed transmitted power to the antenna gain and therefore in order to be able to send at the maximum allowed power, the antenna gain need to be equal to or larger than 51dBi [15].The allowed ERIP is reduced by 2dB for every dB that the antenna gain is less than 51dBi [15]. In Japan the maximum allowed antenna gain is 47dBi [1] and in some countries this value is even lower , hence the antenna design is dependent on the country it will be used in. The specification of the antenna to be

designed in this work is summarized in table 3.1. The antenna will be used in a 60GHz point-to-point link for 10GE (10Gbps Ethernet) designed by SUNNY WAVES. The requirements in table 3.1 are typical and similar to specifications on available 60GHz point-to-point links in the market, but the required antenna gain is however modified by considering the new FCC rules and regulations to suit the our specific system.

In this project the target antenna gain is 47dBi. Because the antenna to be designed is an array, the gain can be scaled by changing the physical size of the array. However, increasing the gain is only possible if the loss introduced by enlarging the antenna dimension is less than the added gain.

Table 3.1 Antenna specifications

Frequency of operation	57-64 GHz
Bandwidth	7 GHz
Antenna gain	45-58 dBi
Polarization	Horizontal/vertical
Pointing direction	Broadside
Return loss	< -10dB

3.2 Survey of antenna candidates

Microstrip antennas have a thin profile and can be fabricated cost-effectively but the high dielectric (substrate) loss at high frequency and narrow bandwidth makes them less attractive in applications where high gain and large bandwidth are desired. Different types of waveguide slot arrays are attractive candidates due to low losses and low cross-polarization level.

Recently, Antenna group at Chalmers has been working on V-band antennas, such as SWE Gapwave antenna (Sheet Waveguide Element Gapwave antenna) [16]. The proposed antenna operates over a wide band and has a thin profile and can be manufactured cost effectively. The tapered E-plane power distribution is performed by utilizing E-bend power divider, and H-plane power distribution is carried out using a parallel plate waveguide reflector. The sheet waveguide elements have lower ohmic loss compared to standard waveguides due to the larger width. The problem of having higher order modes in the wide waveguides is avoided by using sheet-gap-waveguides instead. The primarily results for $140\times140\times30$ mm^3 SWE antenna array without the pin structure are, 37.2 dBi directivity in both E- and H-plane and -12dB reflection coefficient over 50-70GHz. The sidelobe level in both E- and H-plane does not satisfied ETSI class 3B requirements but the author believe that applying the pins can solve the problem.

A slot array antenna which utilizes air gap waveguide as feeding structure has been proposed in[17]. Pyramidal shape pins are used for parallel plate stop-band which are more suitable for applications with frequency above 60GHz. Due to the wide bandwidth of this structure, MMICs can be integrated to the gap waveguide while the radiating slots are placed in the top metal wall. This antenna has the advantage of having high bandwidth, low loss, being cost effective and avoiding MMIC packaging resonance problem.

An E-band double layer 16×16 slot array was designed and fabricated by diffusion bonding of copper plates with satisfactory result in Japan [18]; the gain was measured to be 32.4dBi and the bandwidth was 9%. The antenna showed an efficiency of 83%, and high cross polarization discrimination of -37dB was measured. The architecture of the antenna and the fabricated antenna can be seen in figure 3.1.

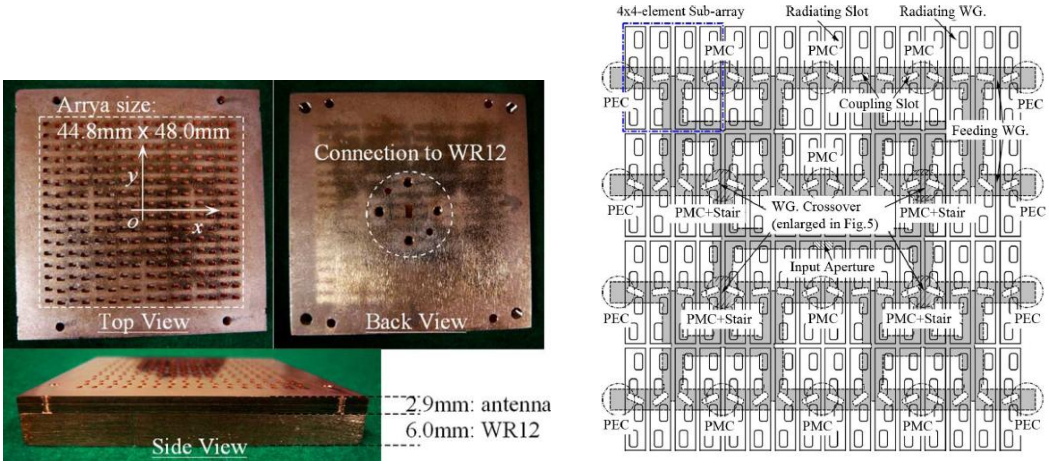

Figure 3.1 The fabricated double layer 16×16 slots array (left) and the architecture of the array(right).[18]

Another double layer slot array for 38GHz point-to-point system with 32dBi gain is designed in [19]. This antenna is also fabricated using diffusion bonding of laminated copper plates. The sub-arrays in this design consists of 10×10 elements and the achieved bandwidth is about 1.5GHz. In the figure 3.2 the architecture of the antenna and the fabricated antenna are shown.

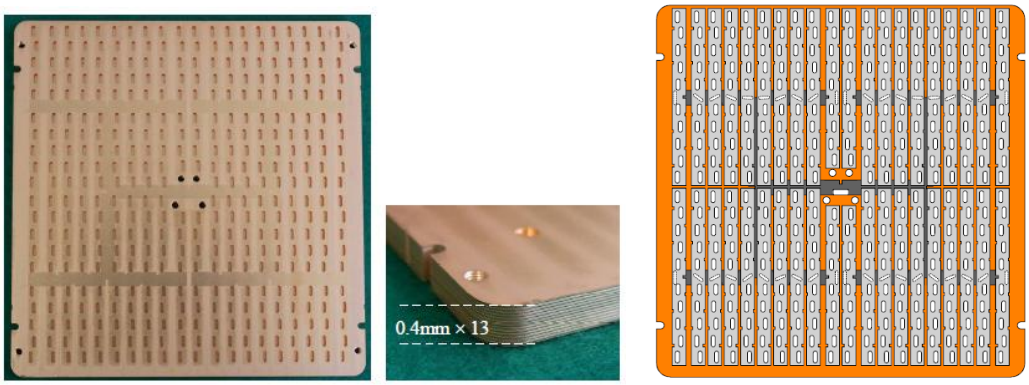

Figure 3.2 The fabricated double layer 20×20 slots array (left) and the architecture of the array(right).[19]

A 16×16 element slot array has utilizing 2×2-element sub-arrays is designed in [20]. The antenna is a double layer structure and the radiating slots are placed on cavities which are feed through coupling slots from the power dividers. The geometry of the antenna and the return loss are shown in the figure 3.5. The reflection bandwidth of VSWR<1.5 is 20.4%. This antenna has also been fabricated using diffusion bonding.

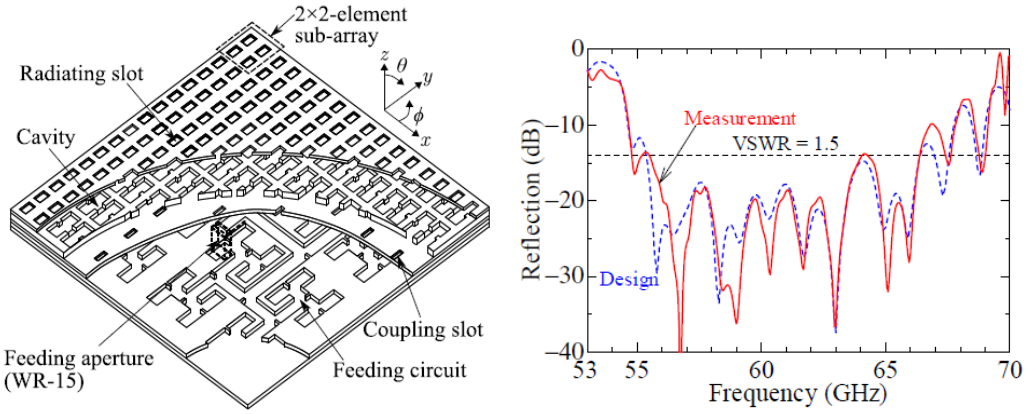

Figure 3.3 The architecture of the array (left) and frequency characteristic of reflection of the array (right).[20]

The different antenna technologies that have been discussed here are all attractive for the design. But planar slot array in rectangular waveguides was chosen to work on because it is a mature technology and have potential for mass productivity, additionally this antenna type required least optimization time.

3.3 Array dimension

In order to calculate the size of the array, the equation 2.2.3-4 for planar array with no grating lobes are used. Here high polarization efficiency of about 100% is assumed due to the fact that the slotted waveguide arrays have very low cross-polarization levels. Another necessary assumption to make is the antenna radiation efficiency which is assumed to be 70% ; this is by considering the fact that the dielectric material is air and the conducting surfaces are of copper which

has high conductivity. By making the latter assumption the required directivity can now be calculated from equation 2.2.5 to be 48.55dBi according to the following calculation.

$$D = \frac{G}{0.7} = 47dBi + 1.55dB = 48.55\ dBi$$

Now using the first assumption and equation 2.2.4 the maximum directivity is calculated.

$$D_{max} \sim D = 48.55\ dBi$$

The required area A is calculated by equation 2.2.3 according to:

$$A = \frac{D_{max}\lambda^2}{4\pi} = 0.143\ m^2$$

Thus for a square array the width w is found by taking the square root of the area A.

$$w = \sqrt{A} = 0.377\ m = 37.7cm$$

3.4 Waveguide dimension

The waveguide dimensions used in simulations for investigating the performance of the slot arrays are the same as the standard waveguide WR-15 for V-band which ranges from 50 to 75GHz. This waveguide has its cutoff frequency for dominant TE_{10} mode at 39.9GHz, and its inner dimensions are 3.8mm ×1.9mm [4]. However in the final design, each component of the antenna utilities waveguide dimensions that suits the components best.

3.5 Slot dimensions and positions

In this section the slot width is discussed and simulations on a resonance type 4-slot array with different slot widths are carried out. The positions of the slots on the waveguide are also calculated theoretically. Figure 3.4 illustrates the 4-slot waveguide array.

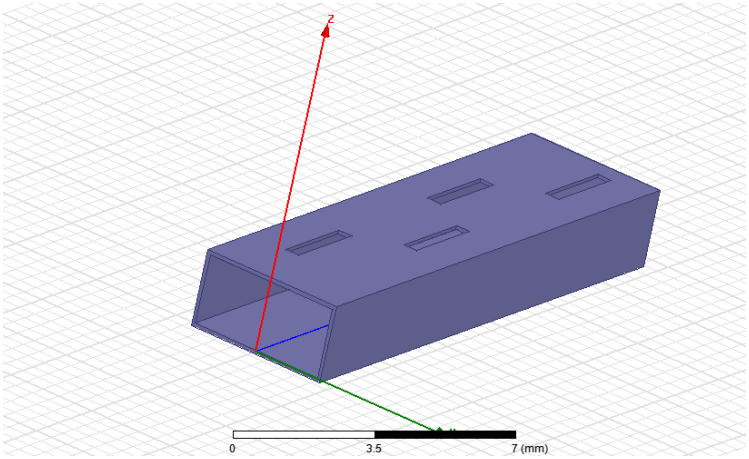

Figure 3.4 A 4-slot rectangular waveguide array

The positions of the slots along the length of the waveguide are chosen to be at the standing wave peaks, the guided wavelength in the waveguide is calculated from 2.3.6 according to:

$$\lambda_{g10} = \frac{\lambda}{\sqrt{1-(\frac{\lambda}{2a})^2}} = \frac{5\text{mm}}{\sqrt{1-(\frac{5\text{mm}}{2\times 3.8\text{mm}})^2}} = 6.4\text{ mm}$$

The last slot should be placed a quarter wave length (guided wavelength) away from the waveguide short circuited end to sit on the standing wave peak; this also makes the input impedance seen from the last slot to be infinite. In addition in order to have the same phase at each slot, the neighboring slots are placed at each side of the broad wall centerline as can be seen in the figure 3.4.
For rectangular slots the slot displacement *d* from the centerline is calculated from expression 2.4.4 to give the total radiation conductance of the 4-slots equal to unity according to :

$$d = \left(\frac{a}{\pi}\right)\sin^{-1}\sqrt{\frac{\frac{1}{4}b\lambda}{2.1\,a\lambda_g\cos^2\left(\frac{\pi\lambda}{2\lambda_g}\right)}}$$

$$= \left(\frac{3.8\text{mm}}{\pi}\right)\sin^{-1}\sqrt{\frac{0.25\times 1.9\text{mm}\times 5\text{mm}}{2.1\times\ 3.8\text{mm}\times 6.4\text{mm}\times\cos^2\left(\frac{\pi\times 5\text{mm}}{2\times 6.4\text{mm}}\right)}}$$

$$=\ 0.93\text{ mm}$$

The simulation shows however that *d=1mm* results in much better matching.

The width of the slot, as mentioned in the background chapter makes a tradeoff between the bandwidth and the cross-polar performance. In order to investigate the influence of the slot width on the bandwidth and co- and cross-polar levels and

be able to choose a proper value, the small slot array in figure 3.4 is simulated for different slot widths. The co- and cross-polarizations are plotted with Ludwig's third definition for a Y-polarized antenna (slot width along y-axis). According to this definition the co-polar and cross-polar unit vectors are:

$$\widehat{co}(\theta,\varphi) = \sin\varphi\hat{\theta} + \cos\varphi\hat{\varphi}$$

$$\widehat{xp}(\theta,\varphi) = \cos\varphi\hat{\theta} - \sin\varphi\hat{\varphi}$$

Thus the magnitudes of the plotted co- and cross-polar components of the electric far field function are:

$$|E_{co}| = \left|E_\theta \sin\varphi + E_\varphi \cos\varphi\right|$$

$$\left|E_{xp}\right| = \left|E_\theta \cos\varphi - E_\varphi \sin\varphi\right|$$

In our simulations the variable *s-width* is slot width and *d* is the slot displacement from the waveguide center line. The plot on the figures 3.5 shows the return loss for different slot widths and two different slot displacements. The co- and cross-polar patterns are plotted in the figure 3.6. In this simulation the width of slots grows toward the centerline to avoid further excitation.

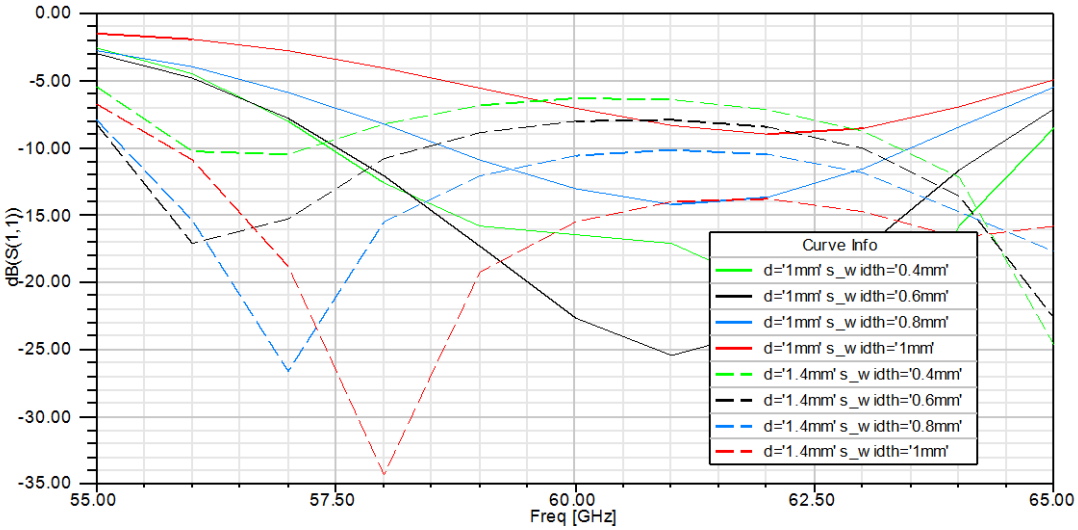

Figure 3.5 Return loss for the 4 slot array with different slot width and slot displacement

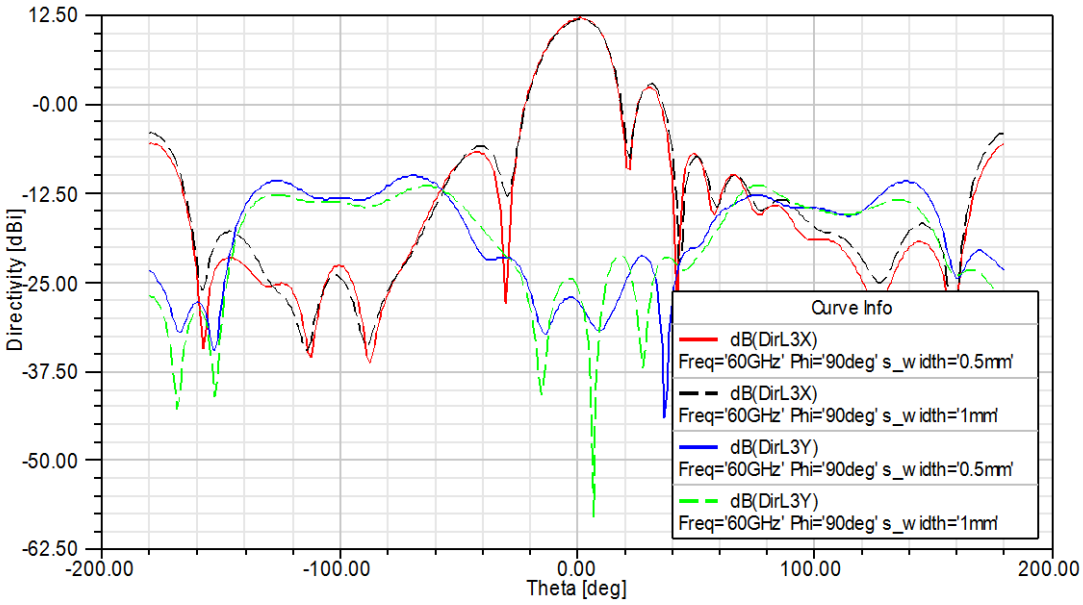

Figure 3.6 Co- and cross-polar patterns for different slot widths (4 slot array)

The plots in the figure 3.5 indicates that for a short slot array (4-slots array), increasing the slots widths more than about λ/10 does not increase the bandwidth of the array and instead effects the matching negatively. This is true for the case when the slot displacement *d* is chosen for best matching. According to the plots (dashed lines) when excitations are further increased (lager *d*) the array shows more bandwidth to the expense of poorer matching. In such case increasing the slots widths more than λ/10 (to about λ/5) are beneficial in terms of both matching and bandwidth. The cross-polar level in the direction of the main beam for the slot with 1mm width is around -25dBi which means about -37.5dB discrimination of the cross- polar component. According to the plot the cross-polar level compared to the 0.5mm case is about 2dB higher but has still acceptable level. Thus wide slots can be used without lowering the polarization performance significantly.

According to the figure 3.5, an array with wide and excessively excited slots have larger bandwidth. The radiation pattern of the array with 1mm wide slot and *d=1.4 mm* is plotted for different frequencies in the figure 3.7.

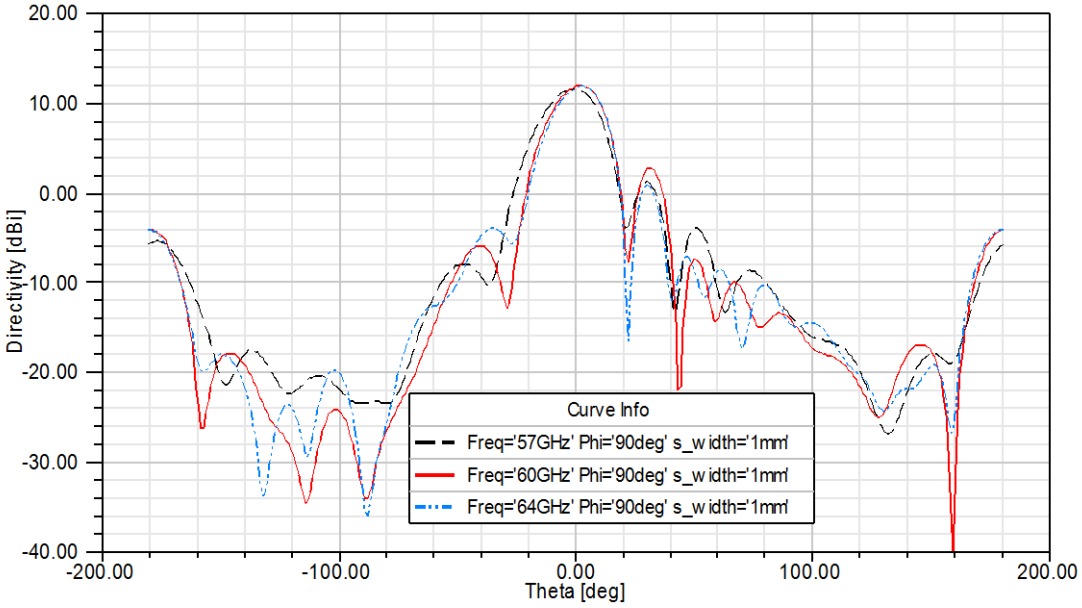

Figure 3.7 Radiation pattern of the 4-slot array for different frequencies

As can be seen in the figure 3.7 the main beam is slightly steered by frequency which can be result of slightly nonuniform power distribution between slots due to excessively exited slots. Because the final array is large, this beam tilting will not affect the final gain much. It can however make the distribution in the final array periodic and cause grating lobes to appear. Thus choice of the slot width and displacement should be carefully done to fulfill both bandwidth and radiation pattern requirements in the same time.

3.6 Slot and waveguide shape

In order to enhance the performance of the antenna and especially its operating bandwidth some other slot shapes which are thought to have benefits compared to rectangular ones have been discussed and simulated in this section. In addition some simple modification, that would not increase the manufacturing complexity, on the waveguide body is also investigated.

The figure 3.8 illustrates a trapezoid slot, this slot can be seen as multiple slots with different resonance lengths on the top of each other.

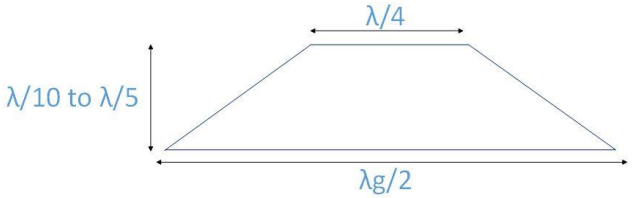

Figure 3.8 A trapezoid slot (figure is not on scale)

The larger dimension is set to a half of the guided wavelength $\lambda_{g10}/2$ and the smaller dimension is set to a quarter free space wavelength $\lambda/4$. The width of the

trapezoid is chosen to be $\lambda/5=1\ mm$. The slot displacement from the center line is chosen to be the same as for the case of 4-slot array (rectangular slots), since a mathematical expression relating the conductance and the displacement for this type of slot does not exist in the literature. The array geometry is illustrated in figure 3.9 and the simulated return loss and the radiation patterns for different slot displacement d2 are shown in the figures 3.10 and 3.11 respectively.

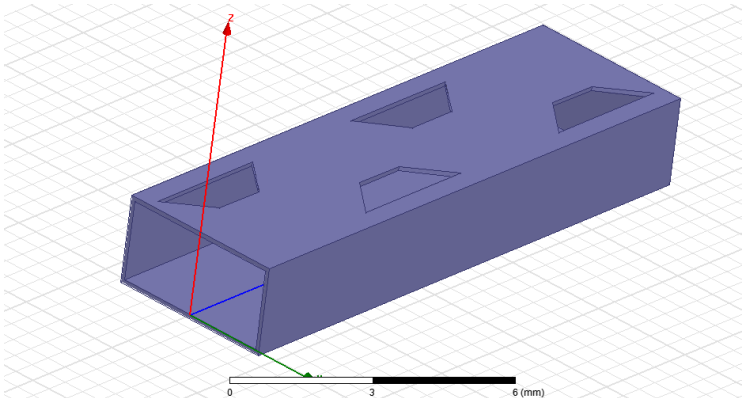

Figure 3.9 Geometry of trapezoid slot waveguide array

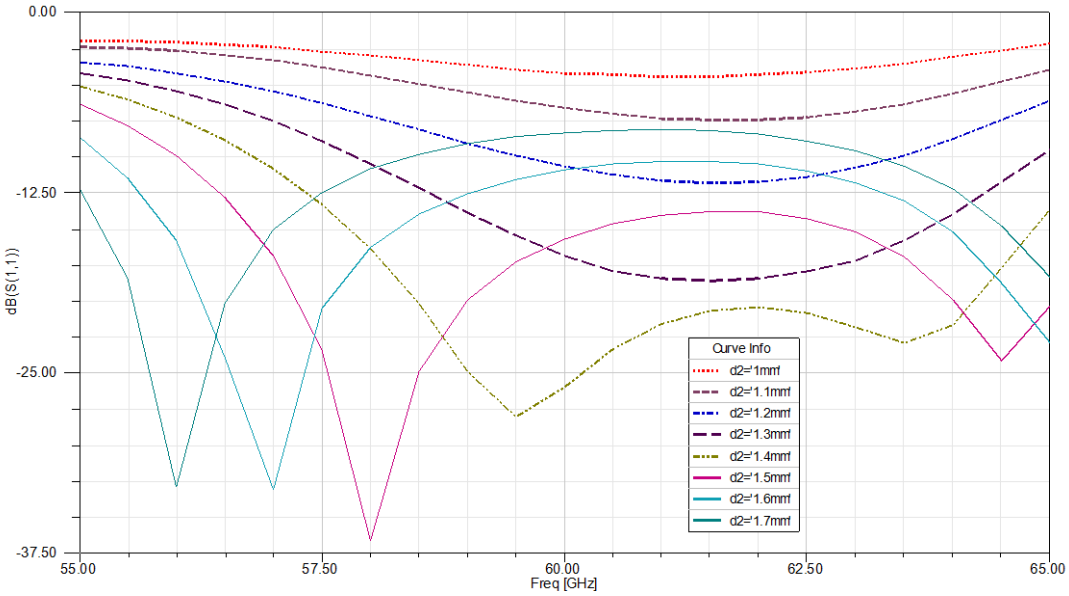

Figures 3.10 Return loss for trapezoid slot array with different slot displacement

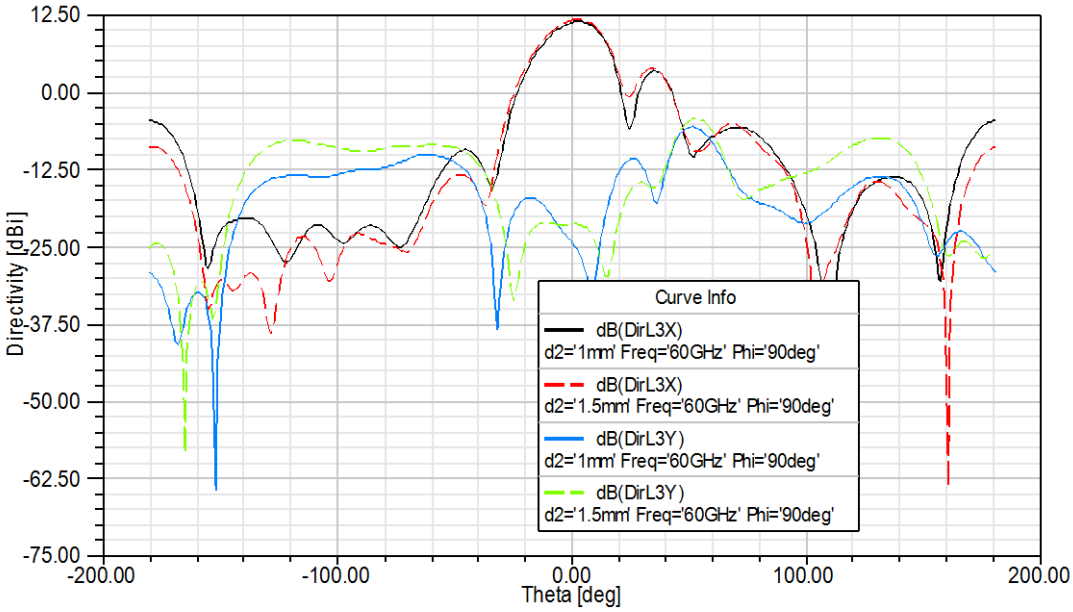

Figures 3.11 Co- and cross-polar levels for trapezoid slot array with different slot widths

The simulation result on the figure 3.10 shows a slightly more wideband characteristic compared to the rectangular slots with the same width and excitation. The polarization performance is almost the same for the two cases at broadside direction.

Next slot shape is the half ridge rectangular slot in figure 2.1.b which is discussed in chapter 2. The dumbbell-slots which have similar geometries as double ridge slots have shown broadband characteristics in many studies. The half ridge slot presumed to have the same broadband property but with better polarization performance. The performance of a half ridge 4-slot array is investigated by simulation. In the figure 2.2 the ratio $s/a = 0.45$ and $d/b = 0.5$ results in $\lambda_c/a = 2.7$. In the figure 3.12 the geometry of the array using half ridge slots is shown. The plot in the figure 3.13 shows the return loss of a ridge 4-slot array with $s/a = 0.45$ and $d/b = 0.5$ for different length a and displacement $d2$.

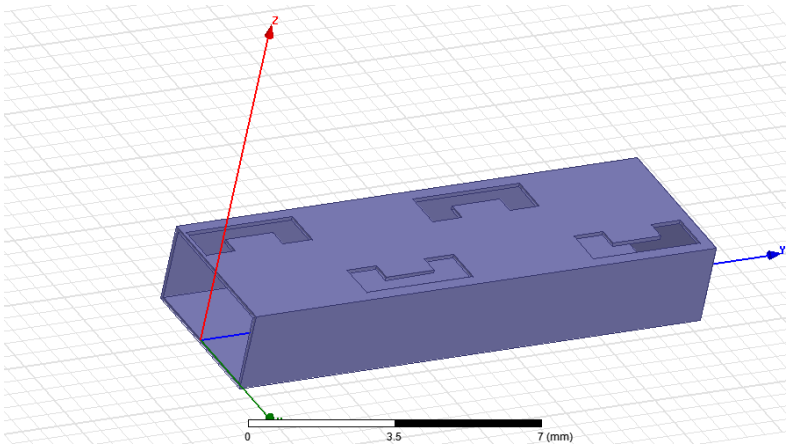

Figure 3.12 Geometry of the half-ridge slot array

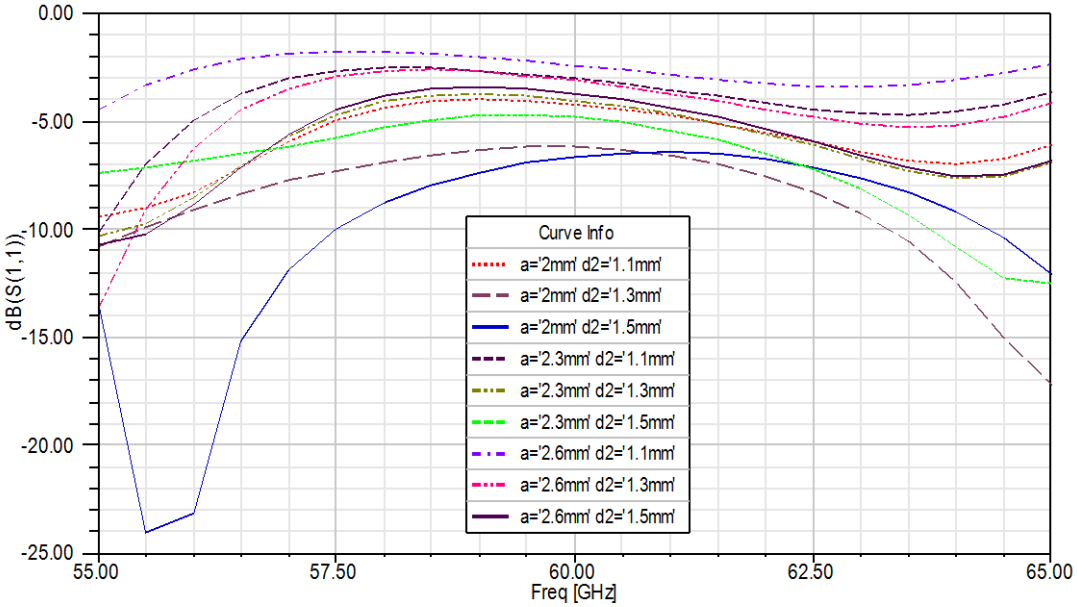

Figure 3.13 Return loss of a half-ridge slot array for different slot lengths *a*

As the plots indicates using half ridge slots causes large mismatching and therefore it is hard to decide if it has broadband characteristics or not. Simulations on 12-slots (both for ridge and rectangular slots) array have also been performed to see if ridge slots show benefits compared to rectangular slots in a longer array; but the results was similar as for 4-slot case.
The conclusion here is that the half-ridge slot shape degrades the performance by causing poor matching, hence it is not a good candidate for our design. It needs to be mentioned that the conclusion here is based on the simulation and the setup that has been chosen; due to the time limitation for this work not all possible variations of the half ridge slot have been examined (for instants the details of the ridge could be varied etc.) and therefore the conclusion applies only for the case that has been examined.

We have seen that the trapezoid slot shape has broadband characteristic, Here the waveguide width *a* is periodically changed (the changes on each wall are exactly opposite to the slots in the same xz-plane) in a way illustrated in the figure 3.14, to see if the bandwidth or matching can improve further. The results of the simulation for different slot displacement *d* are presented in the figure 3.15.

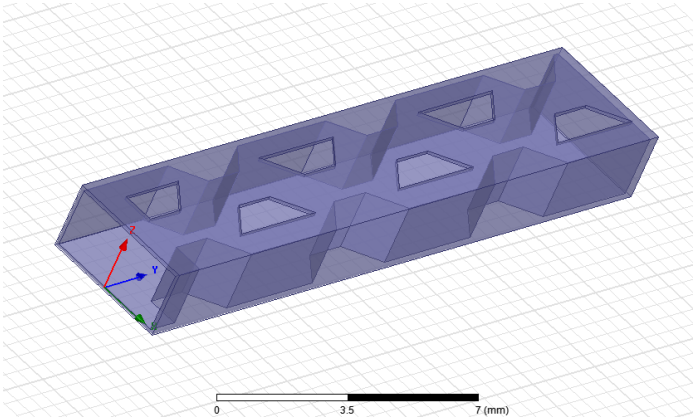

Figure 3.14 Geometry of a trapezoid 6-slot array with waveguide width *a* periodically changed

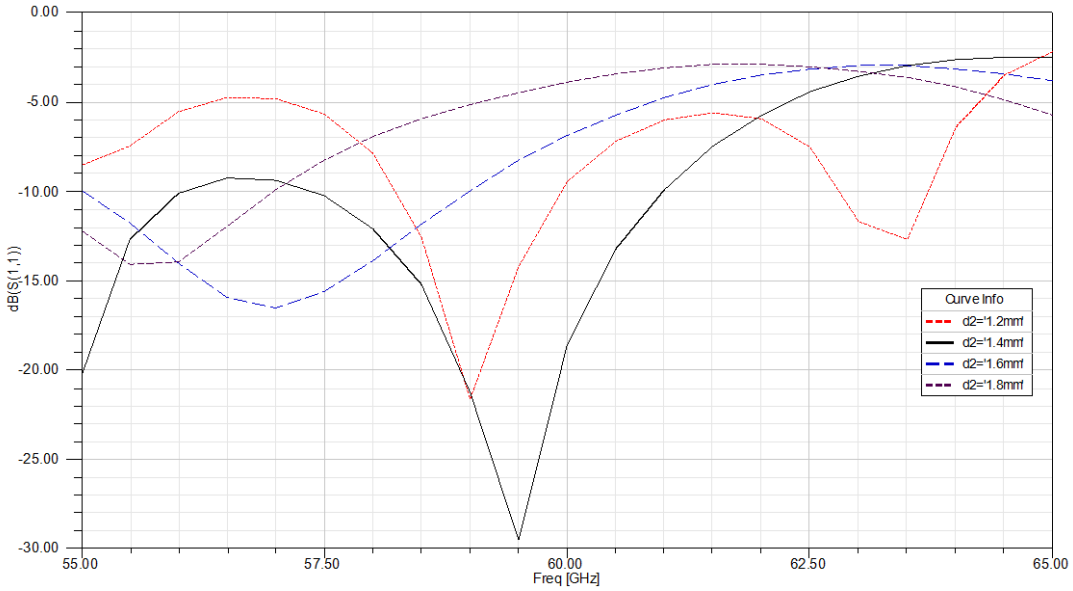

Figure 3.15 Return loss of the trapezoid 6-slot with waveguide width *a* periodically changed

The waveguide shape in the figure 3.14 obviously leads to better matching only for a narrow frequency band and therefore is not beneficial in the design.

It is well known that adding iris in the waveguide improve the matching at least over a narrow frequency band, here the 4-slot array (rectangular slots) with one added iris is simulated for different iris length *i_l* and positions *i_p*. The geometry is shown in 3.16 and The return loss is plotted in the figure 3.17.

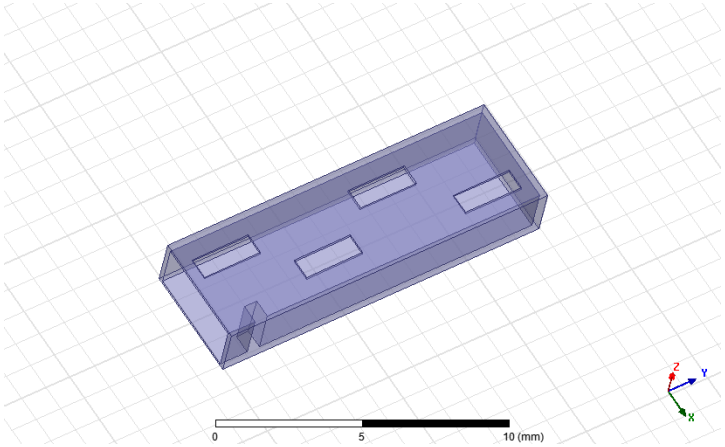

Figure 3.16 Geometry of rectangular slot array with added iris

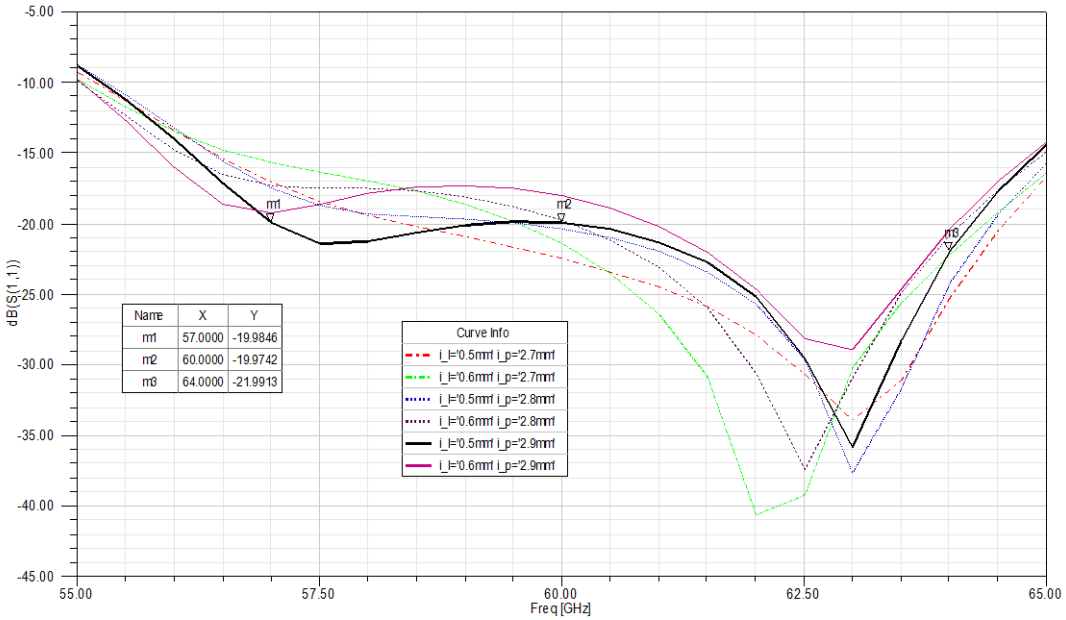

Figure 3.17 Return loss of rectangular slot array with added iris for different iris length and position

According to the plot the added iris leads to much better matching over the entire band of interest and therefore is very attractive candidate for the final design.

3.7 Single layer waveguide slot array with H-plane T-junction feed

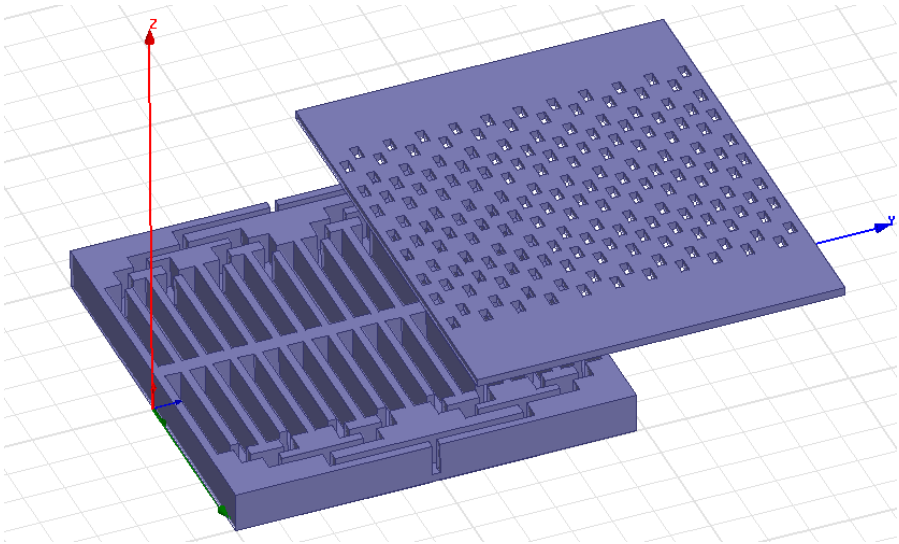

Figure 3.18 Geometry of a single layer planar rectangular waveguide slot array

As mentioned earlier, in order to avoid grating lobes, the element spacing should be less than free space wavelength. In order to achieve that, the waveguides should be placed side by side (along y-axis in the figure) which means no free space for feeding network when many short waveguides are used. Therefore the only feeding option for a single layer waveguide slot antenna is to feed from each end of the antenna. This would work sufficiently good for an small array with less than ten slots per row but not for a large planar array where the waveguides needs to be long with many slots. In a long standing wave array (relative to operating wavelength) with lots of slots the bandwidth is very limited and thus single layer resonance slot array is not an attractive candidate. A partially standing and partially traveling wave array have much better bandwidth. But having partially traveling waves in the waveguide causes phase difference between the slots and therefore tilts the beam. The introduced phase difference is frequency dependent and causes the main beam to steer with frequency. For a large single layer planar slot array of the type that was depicted in the figure 3.18, different regions of the antenna radiates differently and the radiation pattern will be sum of the radiation patterns of these regions. The center of the antenna which contains the standing waves radiates in direction perpendicular to the slots (broadside). The right and left side of the antenna which act as traveling wave arrays, radiates in opposite direction from each other, each with an angle α from the array axis (surface of the antenna). The angle α is given by [1] :

$$cos\alpha = -\frac{\Delta\varphi}{kd_a}$$

where $\Delta\varphi$ is the phase difference from element to element, k is the wave number and d_a is the element spacing. For a waveguide slot array this can be written as:

$$cos\alpha = -\frac{\beta_{10} d_a}{k d_a} = -\frac{\frac{2\pi}{\lambda_{g10}}}{\frac{2\pi}{\lambda}} = -\frac{\lambda}{\lambda_{g10}} = -\frac{\lambda}{\frac{\lambda}{\sqrt{1-(\frac{\lambda}{2a})^2}}} = -\sqrt{1-(\frac{\lambda}{2a})^2}$$

Solving this equation for 60GHz and waveguide dimensions in section 3.3 the angle α is 140degree for the left side traveling array and 40degree for the right side array. Due to the large size of the array the resulting radiation pattern consists of three narrow major beams pointing at 40, 90 and 140degree. Another problem is that in a rectangular waveguide slot array, the element spacing is $\frac{\lambda_{g10}}{2} > \frac{\lambda}{2}$ which cause grating lobes to occur when the main beam is steered.

If the angle α for the two traveling wave parts were close to broadside, the single layer antenna could be a very attractive because it could fulfill the bandwidth requirement and be simple and cost effective at the same time but as the expression above shows the only way to reduce the angle α is to reduce the waveguide dimension; reducing the waveguide width *a* shifts the TE_{10} mode cut-off to higher frequencies but also increases the element spacing which worsen the grating lobes problem.

3.8 Waveguide slot array with separated feed layer (double layer)

In double layer slot array, the top layer contains short slot arrays which are placed along the x- and y-axis to form a large planar array. The bottom layer contains the power dividers; slots on the common surface (coupling slots) feed the short arrays. There are different ways to design this antenna and each has its own benefits and drawbacks. The geometry of our proposed antenna is illustrated in the figure 3.19.

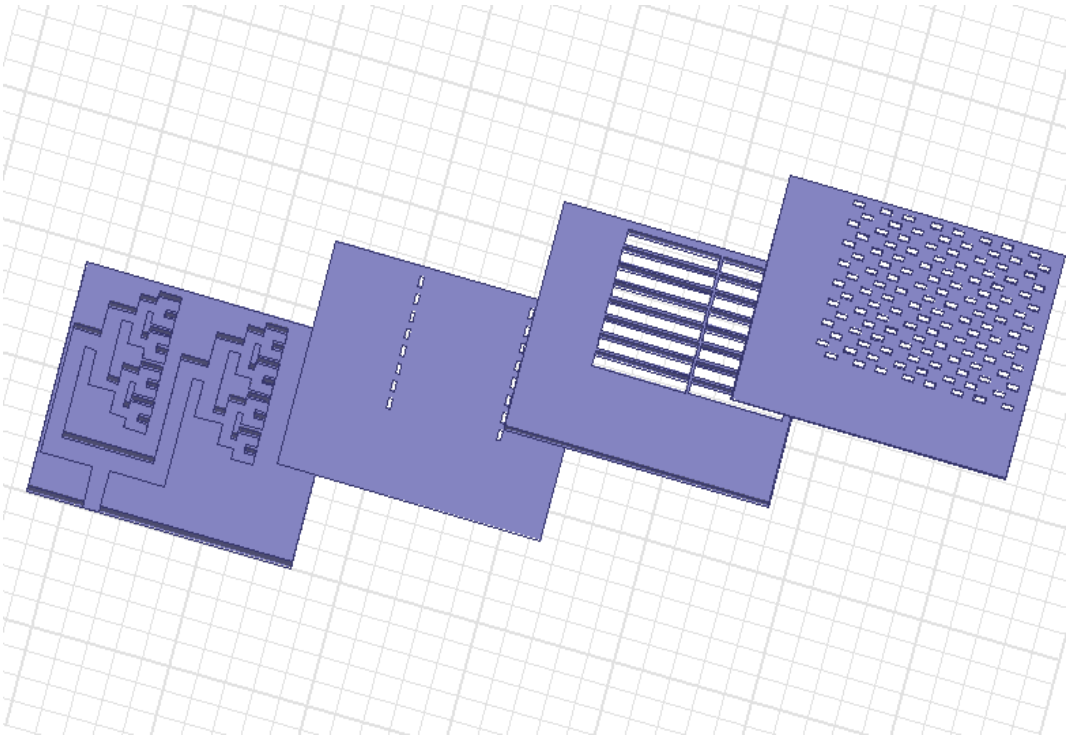

Figure 3.19 Geometry of a planar double layer waveguide slot array antenna utilizing short subarrays (this figure illustrates a small version of the proposed antenna)

In this design the power in E-plane is uniformly distributed through H-plane T-junction power dividers in the bottom layer which feed the short arrays via the coupling slots. The H-plane power distribution is performed by partially by power dividers and partially through the serial-feed structure of the waveguide arrays. This design has the benefit of precise power distribution for E-plane and high bandwidth, but this power distribution network occupies relatively large area and put a limit on how large the antenna can be.

3.8.1 Double layer slot array with 1×8 subarrays

In the following subsections the components of the proposed antenna in 3.19 with 1×8-slot subarrays is designed, simulated and discussed.

3.8.1-1 Design and simulation of 1×8-slot subarray

In order to investigate the wave transition from bottom layer to top layer and examining the performance of the 1×8-slot subarray, the subarray and its feed are designed and optimized together. The cell consists of bottom layer waveguide, the coupling slot and a 8-slot array. The geometry of the cell is shown in the figure 3.20.

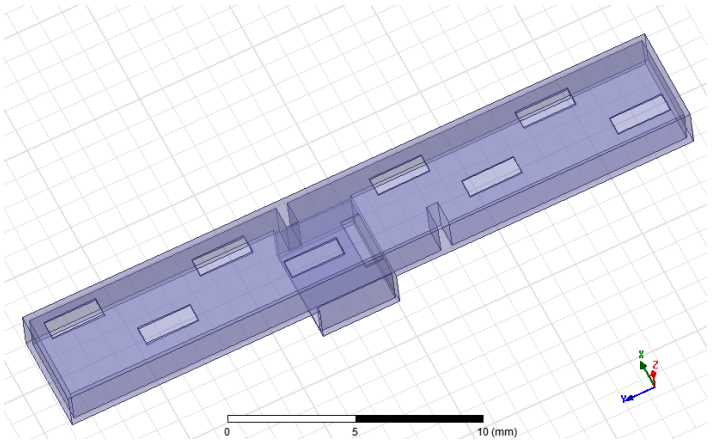

Figure 3.20 Geometry of 1×8-slot subarray with its feed

The distance between two slots in the middle of the subarray is 1.5mm larger compared to all other slots, the distance however is 0.5mm less than the free space wavelength; the coupling slot is placed in this space. The return loss of the subarray for different waveguide heights is plotted in the figure 3.21.

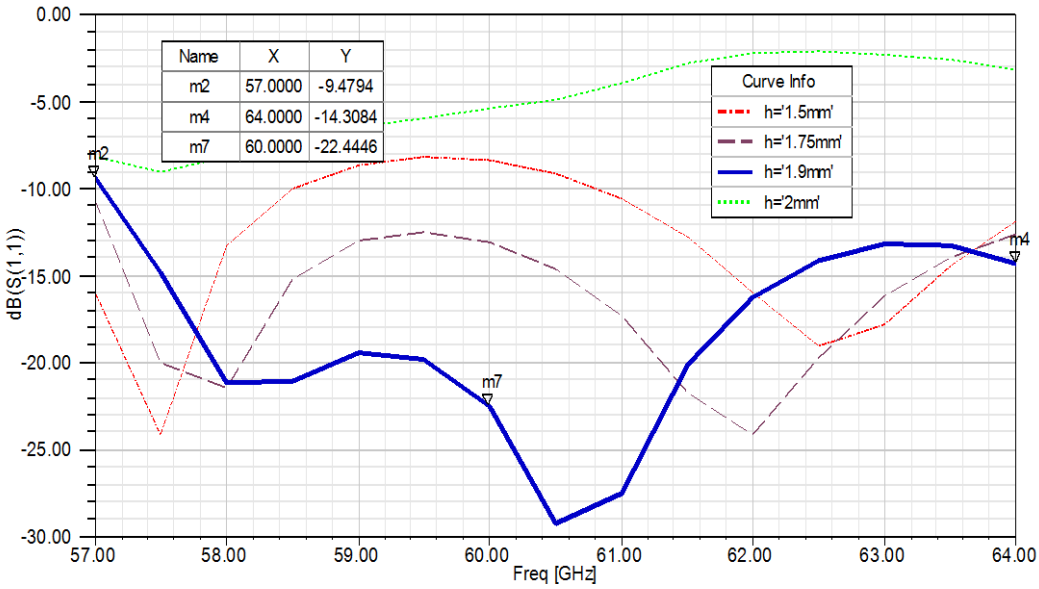

Figure 3.21 Return loss of the of 1×8-slot subarray for different heights

As can be seen in the figure the subarray with *h=1.9mm* has enough bandwidth and the maximum return loss is about -10dB. The parameters of the subarray are summarized in the table 3.2.

Table 3.2 A summary of parameters of 1×8-slot subarray cell

Inner length of waveguide	27.3 mm
Inner width of waveguide	3.8 mm
Slot displacement from centerline *d*	1.2 mm
Slot length *s_length*	2.3 mm
Slot width *s_width*	0.8 mm
Position of iris from the center *i_p*	1.9 mm
Length of iris *i_l*	1 mm
Width of iris *i_w*	0.5 mm
Length of coupling slot *s2_l*	2.3 mm
Width of coupling slot *s_w*	0.7 mm

The radiation pattern of the subarray for center and the upper and lower band frequencies are illustrated in the figure 3.22. As it is shown the main beam, at all the frequencies, points in the broadside which indicates that all slots radiates in phase.

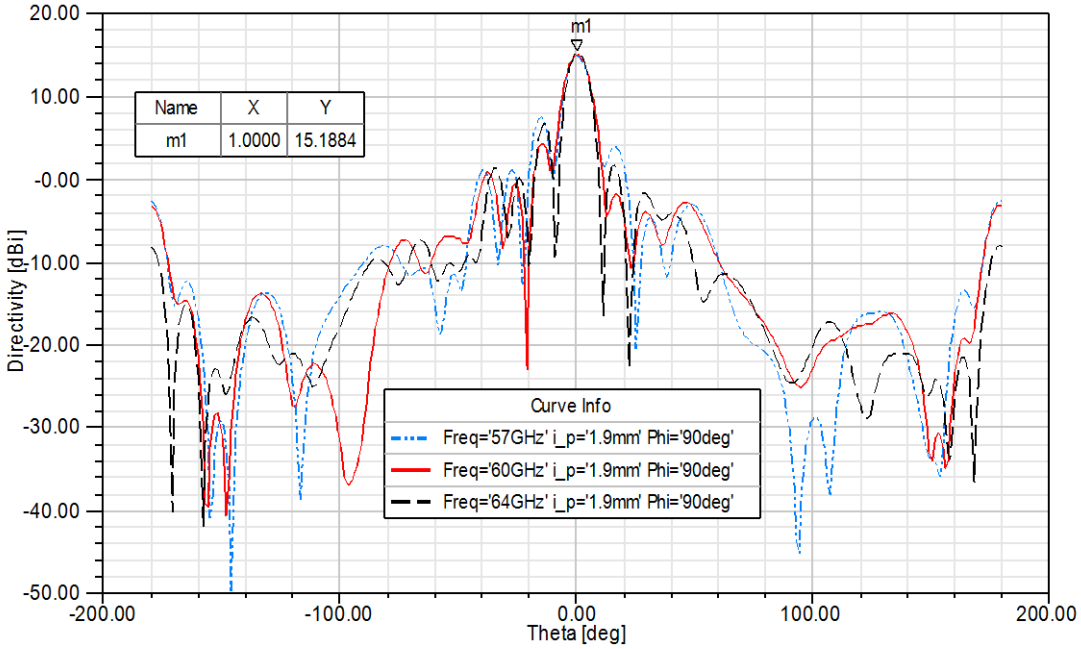

Figure 3.22 Radiation pattern of the 1×8-slot sub array at 57, 60 and 64 GHz

3.8.1-2 Design and simulation of power dividers

As discussed before, in order to meet the requirement on gain, the area of the antenna needs to be 0.143 m^2 but this was only an initial estimation because we did not consider the widths and lengths of the actual waveguides (arrays) that would fill this area. Now by having knowledge of the size of the waveguides (unit cell), the number of waveguides can be calculated from the antenna dimension calculated in section 3.2. The number of waveguides along x-axis (E-plane) is:

$$\frac{antenna\ width}{waveguide\ width} = \frac{377mm}{4mm} = 94.25 \approx 95$$

The number of waveguides along the y-axis when 4-slot array is used is:

$$\frac{antenna\ length}{cell\ length} = \frac{antenna\ length}{subarray\ length} = \frac{377mm}{27.5mm} = 13.7 \approx 14$$

The total number of power divider steps along each axis when 3dB dividers are used is respectively:

$$Number\ of\ divider\ steps\ along\ x_{axis}\ (E_{plane}) = \log_2 95 = 6.57\ \approx 7$$

$$Number\ of\ divider\ steps\ along\ y_{axis}\ (H_{plane}) = \log_2 14 = 3.81 \approx 4$$

The new antenna dimensions with the upward rounded numbers are:

$$w_x = w\ along\ x_{axis} = 2^7 \times 4mm = 512\ mm$$

$$w_y = w\ along\ y_{axis} = 2^4 \times 27.5 = 440mm$$

The space in which the dividers should be placed, is limited to double waveguide length which in our case is *27.5 mm*. As the calculations above indicates 7 steps dividers; one waveguide width needs to be placed there in addition, thus the maximum allowed divider length is :

$$Maximum\ lengthof\ one\ divider\ along\ x_{axis} = \frac{avalible\ space - one\ waveguide\ width}{number\ of\ divider\ steps}$$
$$= \frac{27.5mm - 4mm}{7} = 3.35mm$$

In this design H-plane T-junction power dividers with septum are utilized. Each divider has additionally waveguide bends to guide the wave into desired direction. The last step divider is designed and optimized for the calculated available space (3.35mm). The geometry and return loss are illustrated in the figures 3.23 and 3.24 respectively.

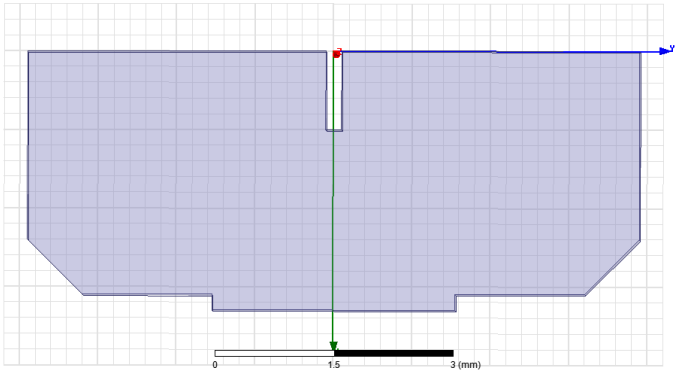

Figure 3.23 The geometry of the power divider

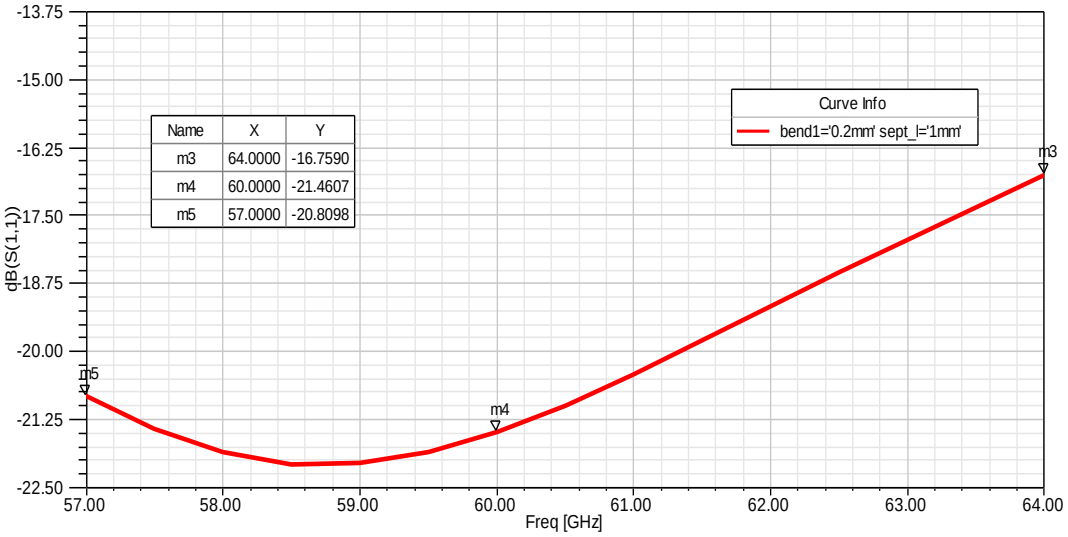

Figure 3.24 Return loss of the designed 3dB power divider

According to the plot the divider has 7GHz bandwidth and maximum of -16.7dB reflection. The parameters of the divider are optimized for lowest return loss and the desired bandwidth. In the table 3.3, the parameters of the divider are summarized.

T able 3.3 is a summary of parameters of the designed 3dB power divider

Inner length of divider (along Y-axis)	3.1 mm
Inner width of divider (along X-axis)	7.8 mm
Wall thickness	0.2mm
Length of septum (along Y-axis) *sept_l*	1 mm
Width of septum (along X-axis) *sept_w*	0.2 mm
Position of septum (along X-axis)	In the center of divider
Bend cut (length of triangle sides) *bend1*	0.2 mm
Simulate return loss @ 60GHz	-16.7dB
Simulated 3dB bandwidth	7 GHz

Tracking the wave along its path from antenna input to the radiating slots, the wave passes through 11 dividers. In order to estimate the total reflection accurately one need to simulated the entire antenna. Due to the large size of the antenna it is not practical to simulate and optimize the entire power division network. Instead a three step divider 1:8 has been designed and optimized to compare with the single divider to estimate the added reflection. The geometry and return loss are illustrated in the figures 3.25 and 3.26 respectively.

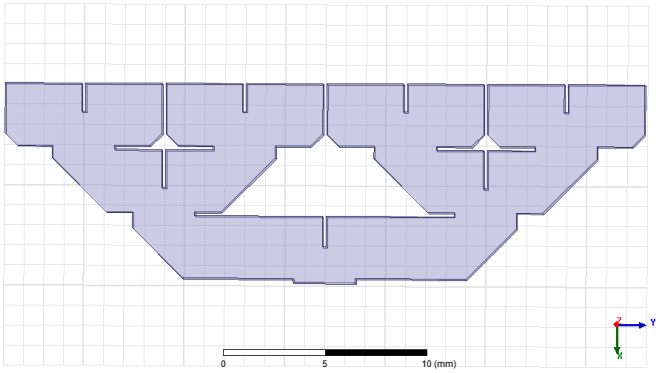

Figure 3.25 The geometry of the three steps power divider network

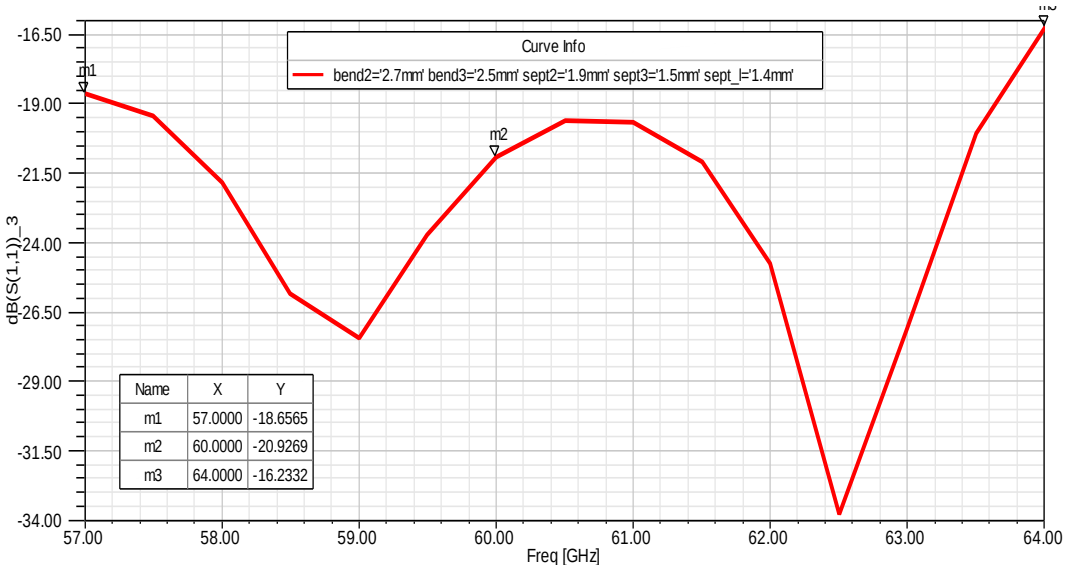

Figure 3.26 Return loss of the three steps power divider network

According to the figure the added reflection is about 0.5dB, thus the total return loss from power dividers is approximately 2.5dB higher compared to the case of a single divider. It is important to mention that this estimation has limited accuracy because the mutual couplings between the radiating slots are not taken into account (when all antenna parts are assembled). However it is possible to fulfill the bandwidth and return loss requirement by tuning the length of the septum and bend of each divider step.

3.8.2 Estimation of final antenna parameters

As mentioned before due to the large dimension of the array it is not practical to simulate the entire array by explicit method (based on FEM). In HFSS version 14 and later versions, there is a powerful tool called finite array DDM which analyze the entire array but reduces the simulation time and required RAM significantly by performing adaptive meshing on a unit cell and using Domain Decomposition. This tool can be used efficiently to simulated the radiation characteristics of the

antenna but in order to estimate the return loss accurately, both layers of the antenna (power dividers and short slot arrays) must be simulated preferably assembled together. A software based on mode matching technique (MMT) can efficiently simulate and tune the power dividers; but such a simulation and tuning is not performed in this thesis.

The procedure of estimating the final antenna performance in this thesis (with the available resources) is as follows:

- Calculating the total loss.
- Performing simulation on a unit cell consisting of two subarrays to account for mutual coupling between two neighboring subarrays and performing final tuning on the unit cell.
- Making an infinite array of unit cells, using periodic boundaries in HFSS, to account for mutual coupling between all elements and estimating the element factor of the array.
- Calculating the array factor in HFSS or MATLAB.
- Estimating the final antenna performance using the array and element factors.

In order to estimate the final gain of the antenna, the total loss needs to be calculated. The losses in a two port network can be measured or calculated by:

$$L = |S_{21}|^2 + |S_{11}|^2 \approx |S_{21}|^2$$

The above expression is used to plot ohmic losses of a 20mm long, air filled rectangular waveguide of cooper for different waveguide heights b . The plot is shown in the figure 3.27.

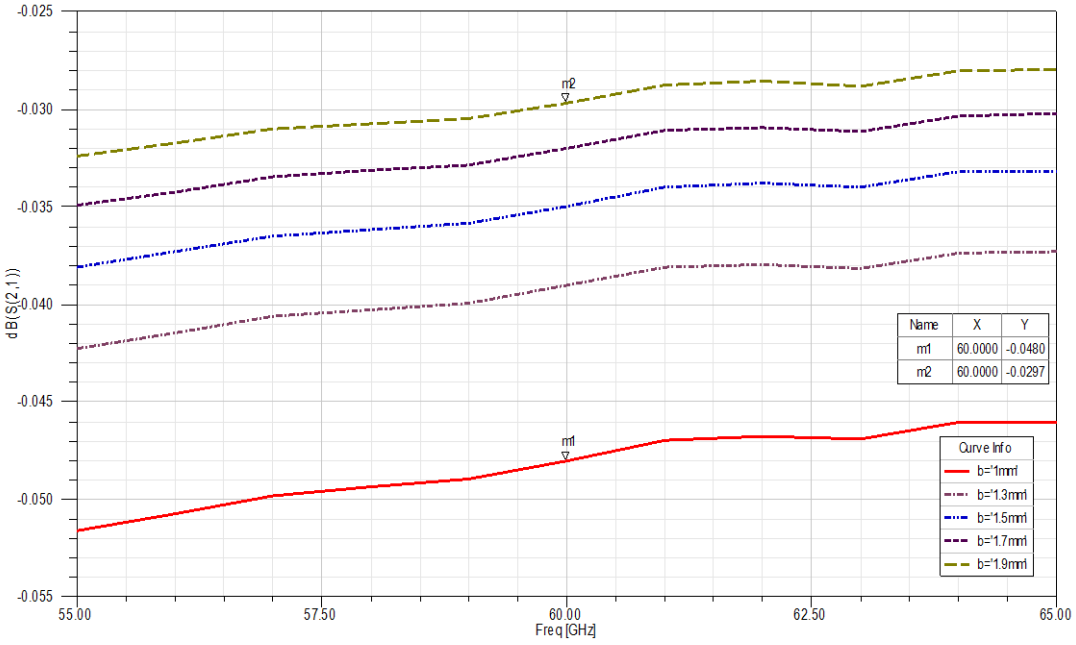

Figure 3.27 Power loss on a 20mm copper rectangular waveguide with different heights

As can be read in the above plot the power loss for *b=1.9mm* is -0.048dB. The attenuation factor in dB is then:

$$\alpha_{dB_{1.9mm}} = \frac{-0.030}{20mm} = -0.0015\,[\frac{dB}{mm}]$$

Another factor that affects the loss in the waveguide is the surface roughness. In our simulations on till now perfectly smooth surfaces have been used which reduces the accuracy of the estimated attenuation. The skin effect at high frequencies causes the majority of current to flow at the surface of the conductor, a rough surface increases the resistivity by impeding the current. The skin dept for copper at 60GHz is :

$$\delta = \frac{1}{\sqrt{\sigma\pi\mu_0\mu_r f}} = \frac{1}{\sqrt{58\times10^6\times\pi\times4\pi\times10^{-7}\times0.999991\times60\times10^9}} = 2.7\times10^{-7}\,m$$

Obviously the skin dept is very low and therefore it is important to include the effect of surface roughness in the loss calculations. There are different formulas in literature which include the surface roughness in attenuation factor. The ANSYS HFSS simulator modifies the material conductivity to include the effect of surface roughness according to:

$$\sigma_c = \frac{\sigma}{k^2} = \frac{\sigma}{(1+e^{\left(\frac{-\delta}{2h}\right)^{1.6}})^2}$$

where *h* is the surface roughness.

An air-filled rectangular waveguide of copper with *b=1.9mm* and *length=1mm* is simulated for different surface roughness to estimate the modified attenuation factor α_c, the results can be seen in the figure 3.28.

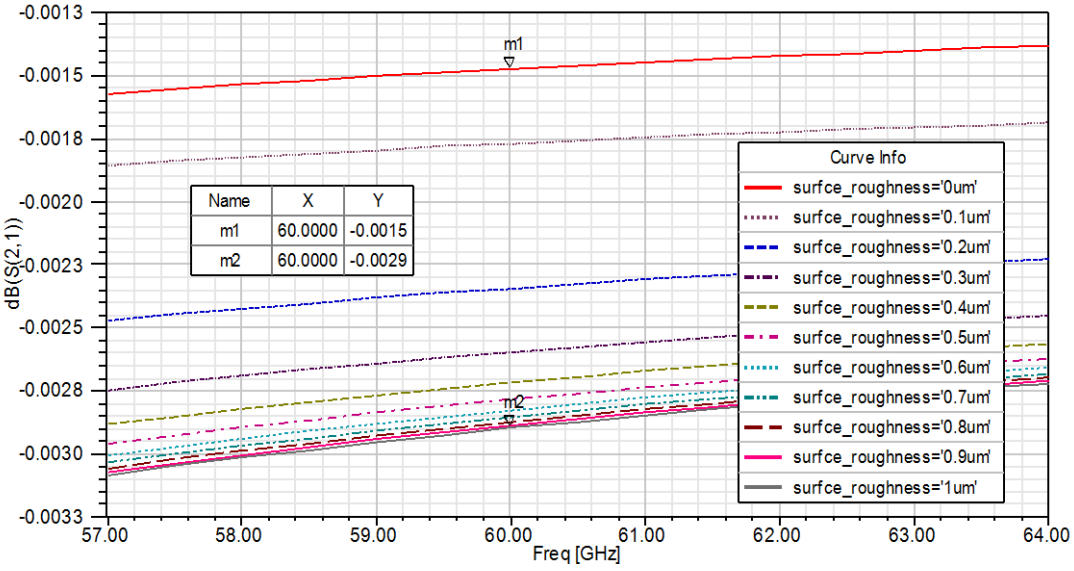

Figure 3.28 Attenuation factor for a rectangular waveguide of copper with *b=1.9mm* and different surface roughness

Now by having knowledge of the wave attenuation per millimeter we can examine if the calculated antenna dimensions tolerate the losses. For that the wave propagation distances from the antenna input to the radiating slots needs to be calculated.

The propagation distance *pl* can be estimated by using the approximate formula below which simply assumes straight path through the dividers instead of following it exactly and then adding the error to the approximated value according to:

$$Propagation\ path\ pl = path\ in\ bottom\ layer + path\ in\ top\ layer\ \approx path\ in\ bottom\ layer$$

$$= \sqrt{(total\ length\ of\ H_{plane} dividers\ )^2 + (\frac{antenna\ width\ along\ x}{2} - \ length\ of\ subarray\ )^2} + \frac{antenna\ width\ along\ y}{2} + \sqrt{(total\ length\ of\ E_{plane} dividers)^2 + (\frac{antenna\ width\ along\ y}{2})^2} + eror$$

$$pl = \sqrt{(4 \times 3.3\ mm)^2 + (\frac{512mm}{2} - 27.3mm)^2} + \frac{440mm}{2} + \sqrt{(7 \times 3.3mm)^2 + (220mm)^2} + (\ (7+4) \times \left(3.3mm + 2mm\ - \sqrt{(3.3mm)^2 + (2mm)^2} \right) = 699.7mm$$

Now the losses in the antenna for largest and smallest attenuation factors $\alpha_{c,max}$ and $\alpha_{c,min}$ will be respectively:

$$L_{max} = \alpha_{c,max} \times pl = -0.0031 \times 700mm = -2.17\ dB$$

$$L_{min} = \alpha_{c,min} \times pl = -0.0015 \times 700mm = -1.05\ dB$$

According to the calculated values the total ohmic loss is between -1.05 to -2.17 dB depending on the roughness of the surfaces. This results indicates that the total ohmic loss is at an acceptable level.

The mutual coupling between the subarrays increases the return loss. In order to determine accurate return loss, the mutual coupling between antenna elements needs to be taken in to account. Therefore a unit cell consisting of two 1×8 subarrays has been created in HFSS and the parameters of the subarray have been tuned for lowest return loss. The results of the simulation can be seen in the figure 3.29.

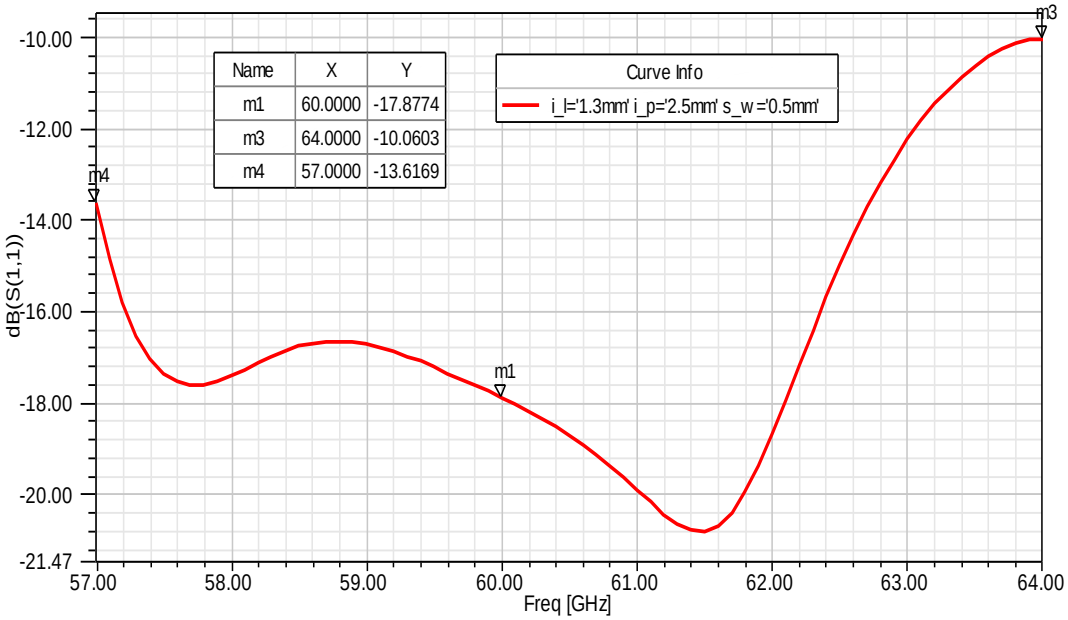

Figure 3.29 Return loss of two 1×8-slot subarrays tuned together

Now using periodic boundaries (master/slave), an infinite array of the unit cell is simulated; the return loss of the cell with all mutual couplings accounted is shown in the figure 3.30.

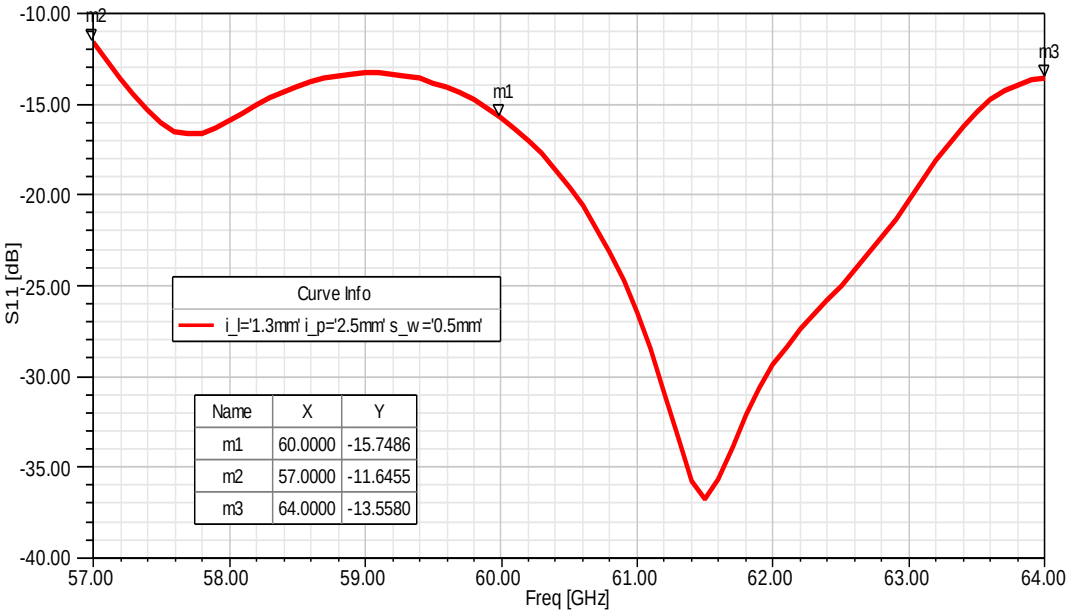

Figure 3.30 Return loss of the unit cell for infinite array

The plot in the figures 3.29-30 are similar thus we can conclude that the return loss of the entire antenna (both layers) is also similar to that of 3.30, hence the loss due to the reflections can be determined to -0.46dB. Adding the ohmic and reflection losses the total loss (ohmic loss and return loss) for the antenna is about 2dB in average.

The element factor of infinite the array, which assumes to be similar to that in our actual finite array, is calculated by using the periodic boundaries of the unit cell. The array factor is calculated in MATLAB for *dx=27.5mm, dy=4.2mm, N=64* and *M=16* at the center frequency. The far field function of the antenna is then calculated by multiplying the array factor and the element factor. The normalized radiation pattern, array factor and element factor are plotted in the figures 3.31 and 3.32 for E- and H-plane respectively.

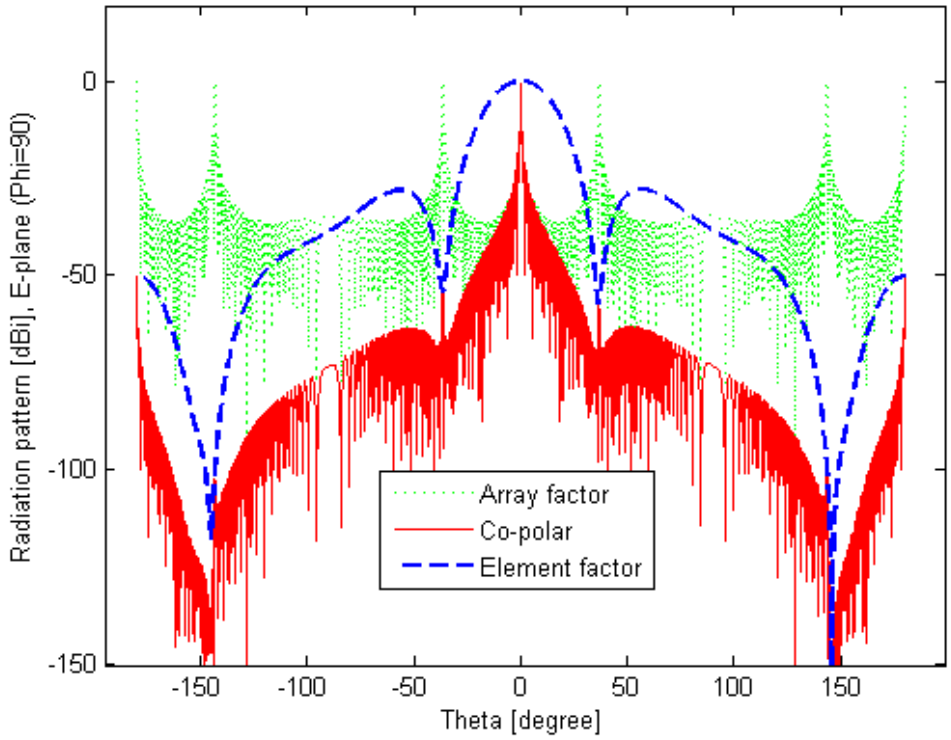

Figure 3.31 Radiation pattern, array factor and element factor in E-plane

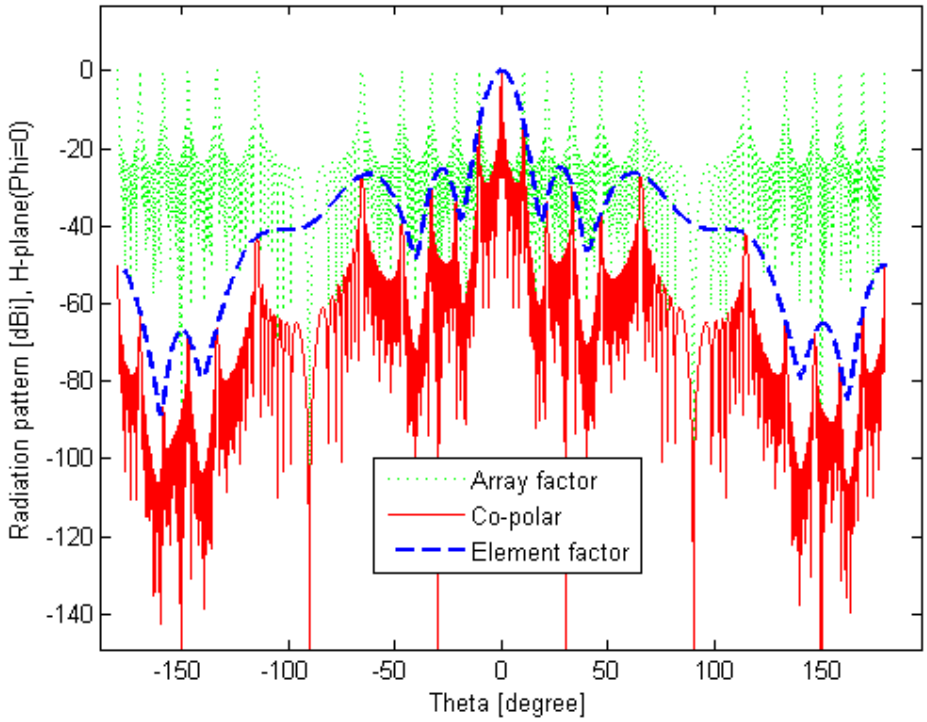

Figure 3.32 Radiation pattern, array factor and element factor in H-plane

The parameters of the antenna are summarized in the table 3.4.

Table 3.4 Summery of calculated antenna parameters

Directivity	47.8 dBi
Gain	45.8 dBi
Beamwidth	0.54 degree
Efficiency	63%
Cross-polarization discrimination	-43dB

In the figures 3.33 and 3.34 the gain in E- and H-plane are plotted and compared with the ETSI RPE(radiation pattern envelop) class 3B requirements.

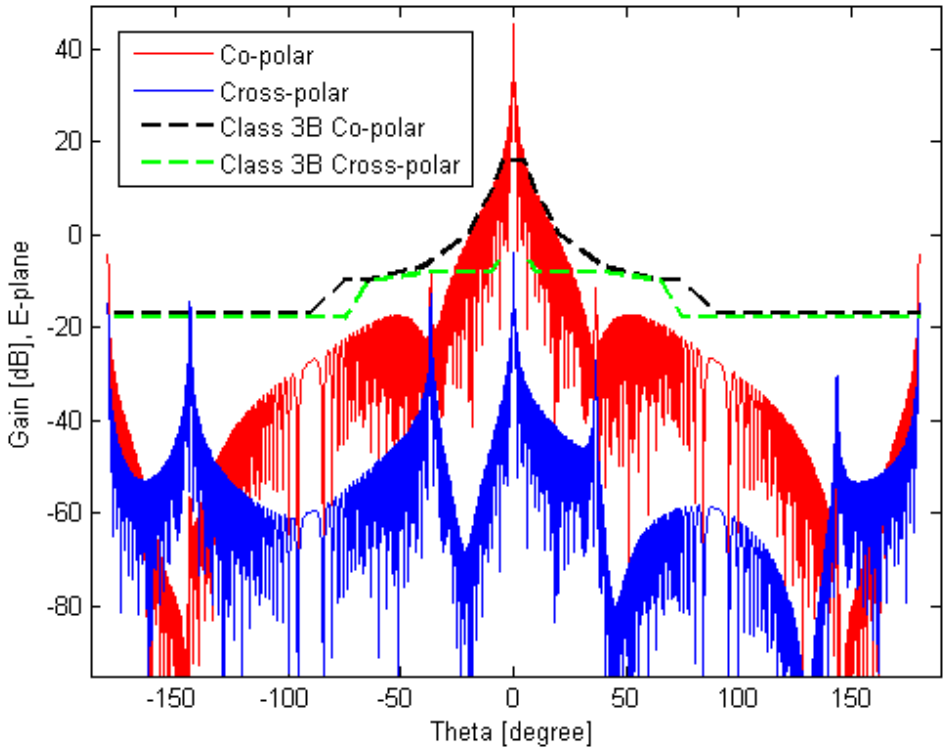

Figure 3.33 Radiation pattern and ETSI RPE requirements in E-plane at 60 GHz

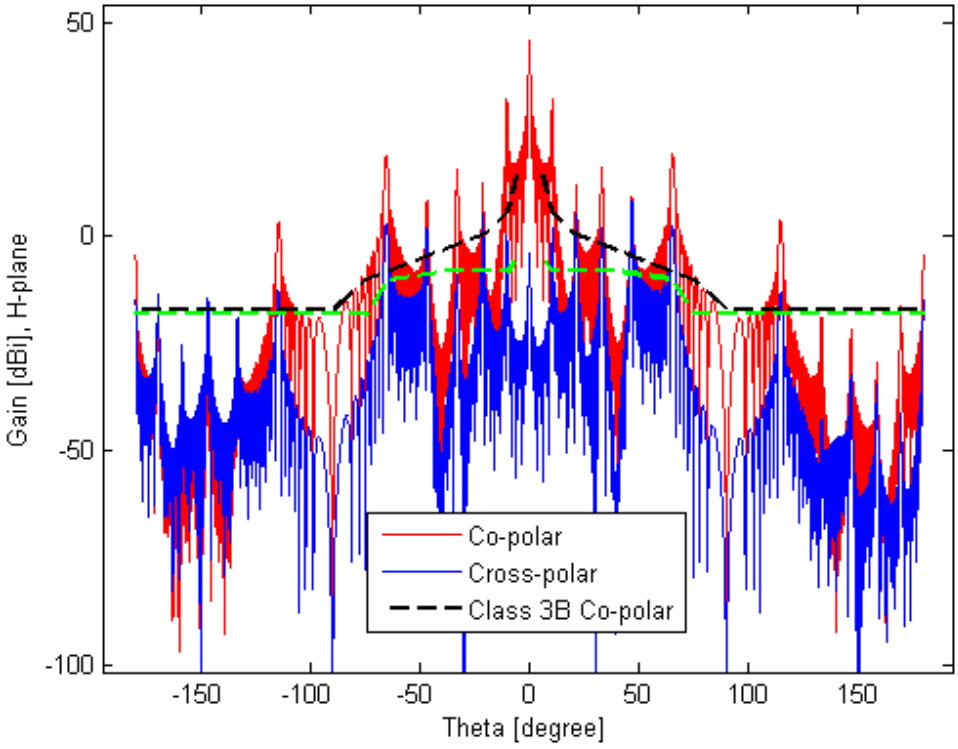

Figure 3.33 Radiation pattern and ETSI RPE requirements in H-plane at 60 GHz

According to the plots the requirements in E-plane are fulfilled but not for H-plane. The radiation pattern in both E-and H-plane shows grating lobes. The ETSI

class3B requirements in E-plane are satisfied but not in H-plane. The grating lobes in the E-plane pattern is however due mostly to numerical errors; the antenna in E-plane utilizes power dividers which contributes to accurate uniform amplitude and phase distribution in this plane and the element spacing is also less than the free space wavelength, thus theoretically no grating lobes should appear. But in H-plane unequal amplitude or phase between the slots in the short arrays causes the grating lobes. Studying the electric field distribution along the unit cell, it was found out that the matching elements (iris) affects the distribution negatively. The grating lobes may be considerably reduced by tuning the iris length and each slot's length and position; but need to be carefully done to not decrease the operating bandwidth. Using the trapezoid slot may also contribute to better amplitude distribution and lower the grating lobes levels. This improvements are out of the scope of this work and will be remained for future work. The ETSI standard is however a European standard, and this antenna will be used in systems operating mostly in North America, but comparing the results with this standard is a good way to evaluate the performance.

Chapter 4

Discussion

In this chapter fabrication of the designed antenna is discussed. In addition integration of a diplexer into the antenna structure, and the possibility of increasing the gain by enlarging the dimensions are briefly discussed.

4.1 Fabrication

One of the main disadvantages of planar waveguide slot arrays is the difficulty of manufacturing the structure. The surface of the array which contains the slots can be simply manufactured by cutting the slot out of a metal plate, the grove structure that contains the waveguides walls can be manufactured by milling. But the difficulty is attaching the two parts, particularly at higher frequencies when the walls are very thin. A solution to the manufacturing problem is to fabricate the antenna using diffusion bonding of thin laminated copper plates. This is a process with high precision and high mass productivity where the thin metal plates with etched patterns are held together under high pressure and high temperature (1300 degrees C). The high pressure and temperature causes the atom from each plate to diffuses to the other and bound the plates[18].

In double layer slot array five etching layers are required. Due to the large size of the antenna and lots of small details, the etching patterns are not shown here. The total height of the antenna is 4.4mm.In order to fabricate the antenna with exact dimensions copper plates with a thickness of 0.1mm is required thus 44 plates are needed. Of these plates 6 will make the top, bottom and middle surfaces and the rest will be used for waveguide walls. If we allow the bottom layer waveguides height to be 2mm and the top layer 1.8mm instead, then 0.2 mm thick plates can be used and this way the number of plates needed will be reduced to a half. In order to see if the designed antenna tolerates this modification, the 1×8 subarray is simulated with these new dimensions. The return loss is shown in the figure 4.1. The power dividers and bends are not significantly affected by changing the height of the waveguide and therefore changed characteristics are acceptable.

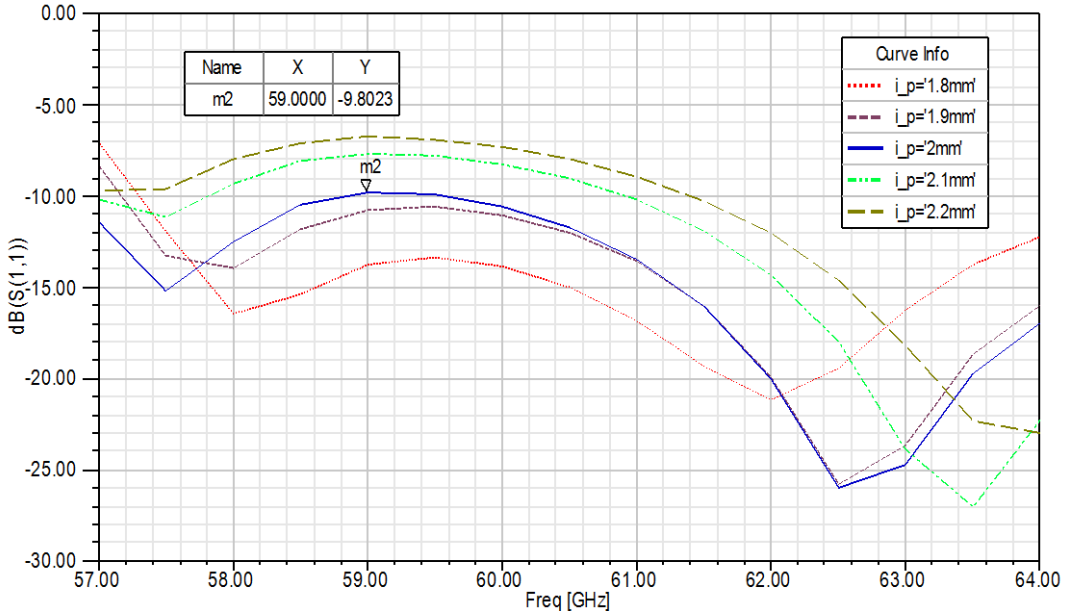

Figure 4.1 Return loss of modified 1×8 subarray for different positions of the iris

As can be seen in the figure 4.1, the brown curve has reflection higher than -10dB around 57GHz but by tuning the position of the iris (blue solid curve) the return loss will be about -10dB for the whole band, thus the modification on the heights can be introduced to the antenna. Tuning other parameters of the subarray can make the reflection even lower but such tuning is not done here and is remained for future work.

4.2 Integrated diplexer

The diplexer is a essential component in transceivers, waveguide diplexers have excellent performance but have the drawback of being bulky and expensive. By integrating the diplexer on the bottom layer of the antenna, one gets this component with almost no additional cost. The disadvantages of integrating the diplexer is that it would require two separated inputs and transmission lines for the transmitter and receiver. A diplexer for separating the channel 57-60GHz and 61-64GHz is investigated briefly. The diplexer consists of three main components, namely, a H-plane T-junction with septum and two bandpass filters. The filters are realized by periodically inserting iris (windows) into the waveguide walls. Due to the large dimension of the antenna, relatively long diplexer can be designed. Millimeter wave H-plane diplexers have been discussed in [21]. The author suggested a modified T-junction which makes the junction as frequency independent as possible; this way the filters and the junction can be designed separately. The geometry of the modified H-plane T-junction is shown in the figure 4.2. The septum width *w* and length *t* should be optimized for maximum bandwidth.

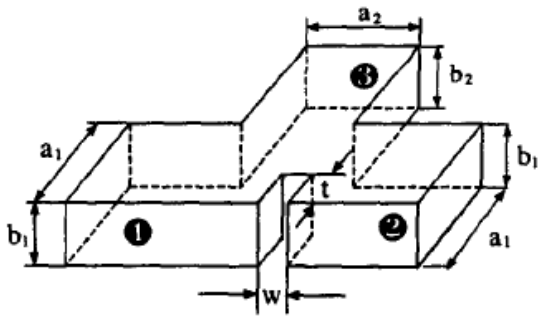

Figure 4.2 Geometry of modified H-plane T-junction[21]

When maximum ripple of 0.2dB and 65dB out off band rejection is required, the minimum filter order for Butterworth, chebyshev I, chebyshev II and elliptical filter is 32, 13, 13, 8 respectively. The amplitude response and the group delay of these filters for the given specification have been plotted using MATLAB and are shown in the figures 4.3 and 4.4 respectively. The MATLAB code can be find in appendix A.

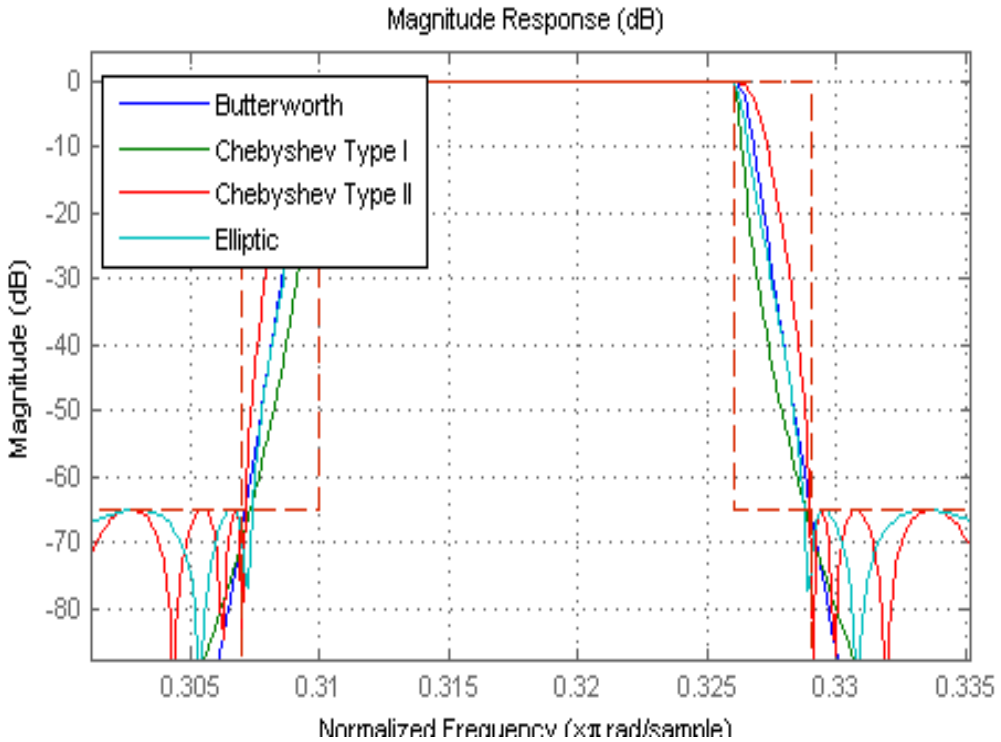

Figure 4.3 Magnitude response of different kind of linear filters with minimum required order

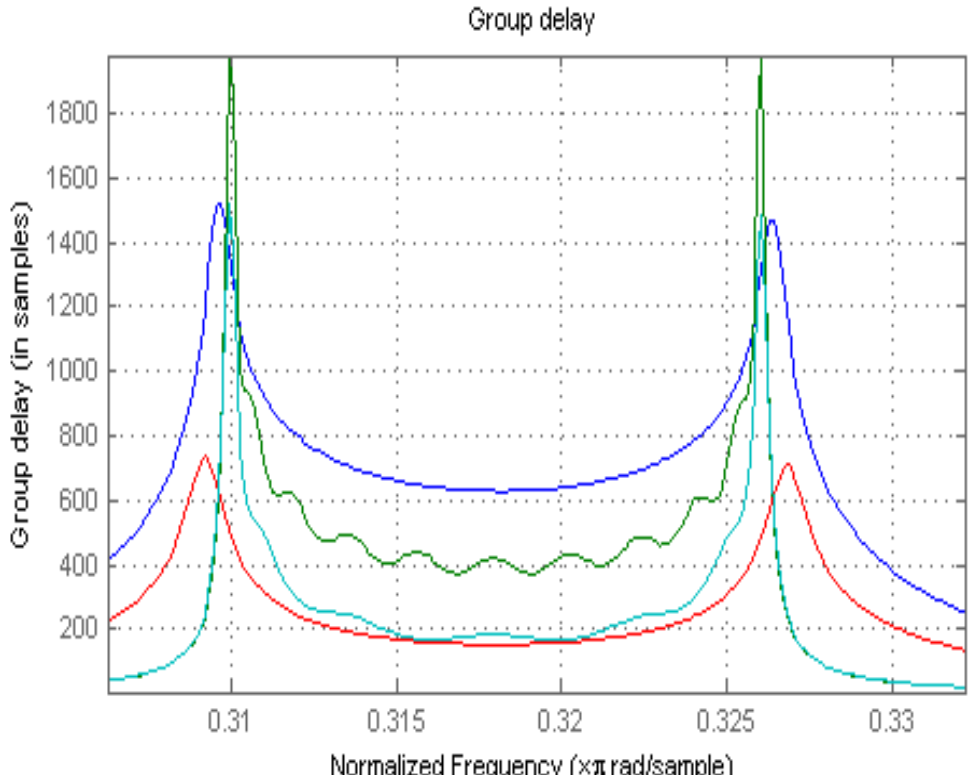

Figure 4.4 Group delay of different kind of linear filters with minimum required order.

The elliptical filter is steepest but Chebyshev II make less distortion to signals in form of group delay. The choice of the filter type is therefore dependent on requirement on signal distortion and the occupied space of each filter section (how large the filter can be).
The design and implementation of the filters in waveguide technology (with iris) and the design and simulation of the diplexer itself is remained for future work.

4.3 Increasing antenna gain

In order to increase the gain, the aperture size of antenna must be enlarged. This statement is true when the loss introduced by enlargement of dimensions is less than the added gain. For instance, in our design, if the dimensions are doubled to increase the gain by 3dB, the propagation path is also doubled *pl=1400mm* which would increase the loss by 1.6dB in average; thus the gain can be increased 1.4dB by doubling the dimensions. But enlarging the antenna dimensions increases the number of required dividers which requires more space. In our design all space under 1×8 subarrays were occupied, thus enlargement of the dimensions is not possible. The problem can might be solved using larger subarrays such as 4×8 elements and utilizing arrays of inclined coupling slots for feeding; the bandwidth however may not be enough. Hence the conclusion here is that the loss for doubling the antenna size is tolerable and the gain can be increased by 1.4dB, but one have to mange to design a 4×8 subarray with enough bandwidth.

Chapter 5

Conclusion

In this thesis high gain planar slot array antenna for 60GHz point-to-point communication has been investigated and a array with 45.5dBi gain has been designed and simulated.

The rectangular waveguide slot array has been investigated to learn about its behavior at millimeter wave frequencies around 60GHz. This study was necessary to find the limitation on maximum length of the array with desired bandwidth. In order to enhance the bandwidth different slot shapes have been studied through simulation results, wide rectangular slots, trapezoid slots and half ridge slots have been simulated. Wide rectangular slots and trapezoid slots showed broadband characteristics but the half ridge slot type miss matched the array and caused high return loss. The wide rectangular slot was finally chosen for the design due to its simplicity to design and fabricate.

The goal was to design a low profile antenna with high performance and efficiency which would have potential for mass production. Therefore the single layer slot array has been investigated first and a partially standing and partially traveling wave solution was suggested. But the gain and bandwidth of the suggested antenna would not meet the requirements for the design.

A double layer slot array was designed, this antenna utilizes short 8-slot arrays with two matching iris on top layer and have operating bandwidth of 7GHz. The power dividers are H-plane T-junction with septum and bends which are integrated in the bottom layer. The antenna is a 128×128 element array and has 45.5dBi gain, 63% efficiency and 11.7% bandwidth ranging from 57-64GHz. The achieved antenna gain is however 1.5dB less than the target gain of 47dBi.The loss calculation in the discussion chapter indicates that 1.4dB gain can be added to the gain by doubling the size of the antenna but this would require design of larger subarrays with different coupling slot arrangement (inclined coupling slot array of 4 slots for instance).The antenna does not fulfill the ESTI class3B requirement in H-plane due to its grating lobes but may be improved by tuning each slot length and position and reducing iris length.

Reducing the grating lobes levels, fabrication and measurement of the antenna, design of the integrated diplexer and an efficient waveguide to antenna transition remains for future work.

References

[1] P. F. M. Smulders, "60 GHz radio: prospects and future directions" *in Proceedings of IEEE Benelux Chapter Symposium on Communications and Vehicular Technology*, 2003, Eindhoven

[2] C. A. Balanis, "Fundamental Parameters of Antenna" in *ANTENNA THEORY: ANALYSIS AND DESIGN*, third edition, New Jersey, Wiley, 2005, pp.44-50

[3] C. A. Balanis, "Fundamental Parameters of Antenna" in *ANTENNA THEORY: ANALYSIS AND DESIGN*, third edition, New Jersey, Wiley, 2005, pp.70-80

[4] C. A. Balanis, "Arrays" in *ANTENNA THEORY: ANALYSIS AND DESIGN*, third edition,New Jersey,Wiley,2005,pp.290-349

[5] P. -S. Kildal "Array Antennas" in Compendium in Antenna Engineering at Chalmers (FOUNDATIONS OF ANTENNAS: A Unified Approach for Line-of-Sight and Multipath), second edition, Gothenburg, Sweden, 2009,pp 419-425

[6] D. M. Pozar, "Transmission lines and waveguides" in Microwave Engineering, third edition, Wiley, 2005,pp 106-116

[7] J. Helszajn, "The Ridge Waveguide "in Ridge waveguides and Passive Microwave Components, The Institution of Engineering and Technology, 2000, London, United Kingdom, pp 1-11

[8] J. Helszajn, "Impedance and propagation in ridge waveguides using the transverse resonant method" in Ridge waveguides and Passive Microwave Components, The Institution of Engineering and Technology, 2000, London, United Kingdom, pp 26-38

[9] P. -S. Kildal "Small Wire and Slot Antennas" in Compendium in Antenna Engineering at Chalmers (FOUNDATIONS OF ANTENNAS: A Unified Approach for Line-of-Sight and Multipath), second edition, Gothenburg, Sweden, 2009,pp 221-231

[10] *MODERN ANTENNA HANDBOOK*, John Wiley & Sons, 2008, pp.97-154

[11] G. S. N. Raju, "*Investigation on slot coupled junctions and radiating slots*, Ph.D. dissertation, Department of Electronics &Electrical Engineering, Indian Institute of Technology, Kharagpur, 1987.

[12] M. Mondal, A. Chakrabarty, "Resonant length calculation and radiation pattern synthesis of longitudinal slot antenna in rectangular*" Progress In Electromagnetic Research Letters*, Vol. 3, 187–195, 2008

[13] R. S. Elliott, *Antenna Theory and Design*, Revised Edition, John Wiley & Sons, 2003

[14] J. C. Coetzee, J. Joubert, W. L. Tan, "Frequency performance enhancement of resonant slotted waveguide arrays through the use of wideband radiators or subarraing," *Microwave and Optics Technology Lett.*, Vol. 22, 35-39, 1999.

[15] Federal Communication Commission FCC, August 9.2013, *Revision of Part 15 of the Commission's Rules Regarding Operation in the 57-64 GHz Band*, February 25.2014, http://www.fcc.gov/document/part-15-rules-unlicensed-operation-57-64-ghz-band.

[16] Jian Yang, "The SWE gapwave antenna - A new wideband thin planar antenna for 60GHz communications", 7th Eur. Conf. on Antennas Propagat. (EuCAP2013), Gothenburg, 8-12 April 2013.

[17] A. Zaman, V. Vassilev, P. -S. Kildal, A. Kishk, "Increasing Prallel Plate Stop-band in Gap Waveguide using Inverted Pyramid-Shaped Nails for Slot Array Application Above 60GHz, 5th Eur. Conf. on Antennas Propagat. (EuCAP), Rome, 11-15 April 2011.

[18] M. Zhang, J. Hirokawa, M. Ando, "An E-Band Partially Corporate Feed UniformSlot Array With Laminated Quasi Double-Layer Waveguide and Virtual PMC Terminations*," IEEE TRANSACTIONS ON ANTENNAS AND PROPAGATION*, VOL. 59, NO. 5, May 2011.

[19] M. Zhang, J. Hirokawa, M. Ando, "Design of a partially-corporate feed double-layer slotted waveguide array antenna in 39 GHz band and fabrication by diffusion bonding of laminated thin metal plates," IEICE Trans. Commun., vol. E93-B, no. 10, pp. 2538-2544, Oct. 2010.

[20] B. Takashi, J. Hirokawa, T. Hirano, M. ando, "A 16×16-element Plate-laminated-waveguide Slot Array with 19.2% Bandwidth in the 60-GHz,"*Proceding of the 2013 International Symposium on Electromagnetic Theory.*,2013.

[21] Y. Rong, H. -W. Yao, K. A. Zaki, T. Dolan, "MILIMETER WAVE H-PLANE DILEXERS,"*IEEE Microwave Theory and Techniques Society*, 1999

Appendices

Appendix A

Matlab code for filter design.

```
%FILTER DESIGN

d = fdesign.bandpass('Fst1,Fp1,Fp2,Fst2,Ast1,Ap,Ast2', ...
   .307,.31,.326,.329,60,0.5,60);% design specification for 57-60GHz filter

Hbutter = design(d,'butter','SystemObject',true);
Hcheby1 = design(d,'cheby1','SystemObject',true);
Hcheby2 = design(d,'cheby2','SystemObject',true);
Hellip = design(d,'ellip','SystemObject',true);

hfvt = fvtool(Hbutter,Hcheby1,Hcheby2,Hellip, 'DesignMask', 'on',...
    'Color','white');
axis([0 1 -70 2])
legend(hfvt, ...
    'Butterworth','Chebyshev Type I','Chebyshev Type II','Elliptic',...
    'Location', 'Northwest')

set(hfvt,'Analysis', 'grpdelay')

%REQUIRED FILTER ORDER
order(Hbutter)
order(Hcheby1)
order(Hcheby2)
order(Hellip)
```